Event generation from effective field theory

Christian W. Bauer[*] and Matthew D. Schwartz[†]

Ernest Orlando Lawrence Berkeley National Laboratory and University of California, Berkeley, California 94720, USA

A procedure is developed for using soft collinear effective theory (SCET) to generate fully exclusive events, which can then be compared to data from collider experiments. We show that SCET smoothly interpolates between QCD for hard emissions, and the parton shower for soft emissions, while resumming all large logarithms. In SCET, logarithms are resummed using the renormalization group, instead of classical Sudakov factors, so subleading logarithms can be resummed as well. In addition, all loop effects of QCD can be reproduced in SCET, which allows the effective theory to incorporate next-to-leading and higher-order effects. We also show through SCET that in the soft/collinear limit, successive branchings factorize, a fact which is essential to parton showers, and that the splitting functions of QCD are reproduced. Finally, combining these results, we present an example of an algorithm that incorporates the SCET results into an event generator which is systematically improvable.

I. INTRODUCTION

To test a model of particle physics we must be able to describe the distribution of particles it predicts. Only a fully exclusive distribution is truly useful, since in order to obtain a meaningful comparison between theory and experiment, the theory must undergo a detector simulation and be subjected to the same cuts as the experimental data. However, high energy colliders produce events with thousands of particles in each event. There is no easy way to describe even the phase space for such complicated final states, and therefore Monte Carlo simulations have become essential for the analysis of every high energy experiment. Practically speaking, the current generation of Monte Carlo tools has been able to reproduce the standard model remarkably well. But with the onset of the LHC, new energy scales and new kinematical configurations, such as events with many high p_T jets, may appear, and these tools will be pushed beyond their validity. So it is our task to help these simulations incorporate as much information from analytical calculations as possible, including loop corrections and the cancellation of infrared divergences when appropriate, while still having them produce exclusive events.

The problem with current techniques is that a number of not necessarily good approximations are forced by practical considerations. For example, it is unreasonable to calculate the analytic expression for a thousand-particle amplitude, and so event generators resort to the parton-shower approximation. This approximation starts with an event resulting in, say, two quarks. These quarks then branch into quarks and gluons, and evolve down in energy until they hadronize at some low infrared (IR) scale. The branching is treated as a classical Markov process with emissions governed by splitting functions derived in the

―――――――
[*]cwbauer@lbl.gov
[†]mdschwartz@lbl.gov

strict collinear limit; thus any quantum mechanical interference effects are lost. A lot of work has gone into improving the results from Monte Carlo simulations. Mostly, it has been directed towards incorporating higher-order QCD effects to improve the distributions in regions where the parton shower cannot be trusted. And, generally, quite good agreement with data has been achieved. However, it remains an extremely important open question to estimate the errors in these techniques, and to be able to reduce those errors systematically. It goes without saying that comparing theoretical predictions to data, or comparing the output of different Monte Carlo schemes, is not the ideal method of estimating error when searching for new physics.

Part of the difficulty in simulating QCD is that it becomes strongly coupled at large distances. But even when QCD is weakly coupled, there is not an obvious perturbation expansion. Of course, we can expand a differential cross section as

$$d\sigma = \sum_n \left(\frac{\alpha_s}{\pi}\right)^n d\sigma^{(n)}. \qquad (1)$$

But when there are multiple scales in the event, such as the relative momentum of pairs of final state partons, large logarithms may appear at any order. Typically,

$$d\sigma^{(n)} = \sum_{m<2n} c_m^{(n)} \log^m \frac{p_i}{Q}, \qquad (2)$$

where p_i is some kinematical variable, and Q is a fixed reference scale, such as the center-of-mass energy of the collision. Even if $\alpha_s \ll 1$ we may have $\alpha_s \log^2(p/Q) \sim 1$ and so the perturbation expansion breaks down. In this case, the large logarithms need to be resummed. Parton showers do this resummation, but without the right framework, it is easy to lose track of which terms are accounted for and which are not. The right framework is an effective field theory which can sum the logarithms, incorporate

finite α_s corrections, and be extended with power corrections to fully reproduce QCD to any desired accuracy. Such an effective theory description was introduced in [1], and in this work we will give more details and expand on that approach.

An effective theory for event generation should not disturb the infrared properties of QCD, where strong dynamics and hadronization take place. Infrared divergences in QCD, such as a logarithmic dependence on the jet resolution scale, can be physical and must be reproduced. These divergences are either soft, for example, when a gluon's energy goes to zero, or collinear, such as when a quark emits a possibly hard gluon in almost the same direction. (SCET) [2–5]. In this paper, we show how SCET can be implemented in an event generator so that the results are systematically improvable. We will demonstrate how at leading order, SCET is equivalent to the traditional parton-shower approach. Parton showers write the probability for a branching as

$$\mathrm{d}\,\sigma = \Delta(\tau)P(\tau, z), \qquad (3)$$

where $P(\tau, z)$ is a splitting function and $\Delta(\tau)$ a Sudakov factor

$$\Delta(\tau) = \exp\left(-\int dz P(\tau, z)\right). \qquad (4)$$

The splitting function represents the probability of a parton to split, and the Sudakov factor accounts for the fact that if a parton splits at a scale τ, it should not have already split. We will see the splitting function derived from collinear emissions in SCET and the Sudakov factor reproduced from renormalization group (RG) evolution. One of the important facts of QCD, which gives rise to parton showers and which allows Monte Carlo techniques simulate multiple branchings, is that a given cross section factors into a product of probabilities, namely, the probability to create an initial final state, multiplied by the probabilities to have subsequent splittings. This will be rederived from SCET.

Besides justifying the parton-shower approach, SCET can be used to improve it. The problem of how to properly combine QCD matrix elements with parton showers is first cast in the language of scale separation. When the logarithms appearing in the differential cross section are large, the scales are widely separated, and the effective theory can be matched at the higher energy scale, and run down to the lower scale. The splitting functions used in the parton shower describe the long distance behavior of QCD (and of SCET), while the short distance physics is different in the two theories. Although the short distance physics of QCD is not fundamentally part of SCET, it can be fully reproduced through a consistent matching procedure. Thus SCET is valid at all scales, in contrast to QCD or the parton shower separately.

We would like this paper to be self-contained and generally readable by both SCET and the Monte Carlo communities, as well as people familiar with neither field. So we attempt to incorporate a terse and incomplete review of event generators in Sec. II and of SCET at the beginning of Sec. IV and in Appendix A. Section III gives a schematic presentation of the general idea of event generation in SCET. As much as possible, we sequester the detailed calculations to Sec. IV, which is the heart of the paper. The results of Sec. IV are applied in various ways in Sec. V. We show first how Sudakov factors are reproduced from the renormalization group in SCET. A discussion is included of next-to-leading log resummation. We then discuss how the splitting functions and the factorization of successive branchings are understood from SCET. Next, we explore next-to-leading order (NLO) effects, which include the cancellation of infrared divergences in physical observables. We show that SCET reproduces the perturbative QCD result for the total inclusive cross section at NLO. Finally, we use the SCET results to calculate some observables from parton-level results. We present the thrust distribution for 3-parton states, and the 2-jet fraction σ_2. Section VI first summarizes how differential cross sections are calculated, and then describes a simple algorithm that can use these cross sections to distribute events in a Monte Carlo program. Finally we present our conclusions and outlook. We also include in Appendix B some kinematical relations and conventions that are used throughout the paper.

II. INTRODUCTION TO PARTON SHOWERS AND EVENT GENERATORS

In this section we review some aspects of how parton showers and event generators work, with an eye towards comparing to the SCET approach. This section contains no new information, and readers familiar with the subject can safely skip this section.

An event is typically generated in three phases [6–9]. First a simple hard process is selected at the parton level, with a probability proportional to its production cross section calculated using the standard Feynman diagram methods. Second, the partons, which are taken to be highly off shell at the hard scale, radiate additional partons and "evolve" down.

Parton showers use classical evolution to describe the emissions of particles: they assign a probability for one particle to split in two. This probability depends on two kinematical variables. The first variable, τ, is chosen to be a measure of the virtuality of the initial particle, and tends to zero if the two final particles are collinear. The second variable, z, measures the relative energy between the two final particles. Using that the splitting is independent of azimuthal angle, and that the branching probability is linearly divergent as τ goes to zero, the probability is proportional to

$$P(\tau, z) = \frac{\alpha_s}{2\pi} \frac{P_{ab}(z)}{\tau} \qquad (5)$$

up to terms of order τ^0. Here, $P(\tau, z)$ is our notation, while P_{ab} is the traditional spin averaged splitting function, with a, b indexing the final state particles. For example, the quark splitting function in QCD is

$$P_{qg}(z) = C_F \frac{1 + z^2}{1 - z}, \tag{6}$$

where $C_F = \frac{4}{3}$.

In order to calculate the classical probability of an initial particle with virtuality τ_1 to branch at a particular value τ_2, one needs to include the probability that no branching has occurred at a larger value of τ. This is similar to the well-known case of nuclear beta decay, where this no-branching probability is responsible for the exponential decay rate. The probability of no-emission from τ_1 to τ_2 is then given by an integral, known as a Sudakov factor

$$\Delta(\tau_2, \tau_1) = \exp\left(-\int_{\tau_1}^{\tau_2} \frac{d\tau}{\tau} \int dz \frac{\alpha_s(\mu[\tau, z])}{2\pi} P_{ab}(z)\right). \tag{7}$$

Here, the scale μ at which α_s is evaluated can depend on both τ and z. As an example, consider a quark-antiquark pair with virtuality Q. The probability that a branching occurs at a scale τ is given by the probability that neither quark branched at a scale greater than τ, times the probability for either of the two to branch at that scale. Thus the differential cross section to have three final state partons is given by the cross section for two final state particles, multiplied by a Sudakov factor and the sum of the two splitting functions for quark and antiquark emission

$$d\sigma_3 = d\sigma_2 \Delta(Q, \tau)^2 [P(\tau, z) + P'(\tau, z)], \tag{8}$$

where P' is the equivalent of P for the antiquark emission.

Parton showers rely on two crucial assumptions. First, one neglects the interference between the emissions off the various particles, and second, the intermediate states are taken on shell when deriving the splitting functions. For example, in the emission of a gluon off a quark-antiquark pair, the square of the full matrix element in QCD is replaced by a sum of two independent emission graphs

$$\tag{9}$$

Both of these assumptions can be justified in the limit $\tau \to 0$, which implies that the virtuality of the branching particle is small compared to its energy. In that limit the branching particle becomes almost on shell and the interference between the two QCD diagrams becomes subdominant.

Note that the two diagrams on the right-hand side are not gauge invariant and thus not well defined. The parton shower circumvents this problem by summing only over physical polarizations, which restores gauge invariance,

ipso facto. The splitting functions are well defined because the residue of the pole is gauge invariant and does not get a contribution from interference. But the τ^0 and higher-order pieces depend on conventions. For example, take the square of the relative transverse momentum between the two final state particles, p_T^2, as the measure of the virtuality τ. The branching probability is then proportional to $P(\tau, z)$ with $\tau = p_T^2$. Now consider the different choice $\tau = t$, where t denotes the invariant mass of the two final state particles $t = (p_i + p_j)^2/Q^2$. These two variables are related by

$$p_T^2 = \frac{t(z - t + tz)(1 - z - tz)}{(t - 1)^2} = tz(z - 1) + \mathcal{O}(t^2). \tag{10}$$

Using this to change variables in $P(t, z)$, we reproduce the same pole terms as in $P(p_T^2, z)$, however the higher-order terms differ. Thus we cannot define the higher-order terms in splitting functions in a consistent way.

From the discussion so far we have learned that parton showers give simple expressions for the emission of partons. These can easily be turned into powerful computer algorithms using Monte Carlo techniques, which can be used to generate final states with many partons. One starts with a cross section for a process with a limited number of particles in the final state. In practice, event generators often start with processes with only two final state partons. The virtuality of these two partons is chosen to be comparable to the hard scale of the interaction Q, and all additional partons in the final state are generated by the classical probabilities of particles to split into two particles with lower virtuality. This can be cast in a Markov Chain process, evolving the system from high to low virtuality, adding additional particles through the splitting functions. Different parton-shower algorithms all use the physics described above, but they differ in which next-to-leading order effects they incorporate. First, they use different choices for the evolution variable τ [10,11]. Second, they use different choices for the scale μ at which $\alpha_s(\mu)$ is evaluated in (7). Finally, for each emission in a parton shower, z and τ are distributed over phase space assuming that the partons are on shell. But subsequent branchings require the partons to be off shell, so there is an ambiguity in how to assign the kinematics [12]. All of these effects only contribute at next-to-leading order, but they can give rise to considerable differences between the different programs in certain cases.

Another aspect of QCD that has to be taken into account carefully arises for the emission of a soft parton [13,14]. The analog of the Chudakov effect from QED is that, when integrated over azimuth, soft emissions at large angle are sensitive only to the aggregate color charge of all the contributing partons. The result is that large angle soft emissions are suppressed. This is generally incorporated into parton showers by either using an evolution variable

which corresponds to angle (as in Herwig [7]) or by explicitly vetoing emissions which are not angular ordered (as in some versions of Pythia [15]).

The assumptions of parton showers restrict their validity to regions of phase space where each successive emission has to have virtuality much smaller than any previous one, $Q \gg \tau_1 \gg \tau_2 \gg \ldots$. Regions of phase space with $\tau \sim Q$ are only correctly described by the full QCD matrix elements. Thus, only an event generator which combines both the full QCD matrix elements with the parton showers will yield predictions which are correct to a given fixed order in perturbation theory, while also summing the leading logarithms correctly and allowing for the additional production of partons with small transverse momenta. Several techniques have been developed which allow such a combination of QCD matrix elements with parton showers, including original work which has been implemented in Pythia and Herwig [16–18] and some more recent developments [10,19–23]. One popular example is the CKKW procedure [19], which provides a way to combine tree-level QCD matrix elements with parton-shower evolution. The idea is to compute the exact tree-level QCD matrix element for an event, including interference, but with a lower cutoff τ_0 on the virtuality between any two particles. One then reconstructs the dominant diagram using the k_T algorithm [24] and reweights the event by multiplying with appropriate Sudakov factors. Parton showers are then added to these matrix elements, vetoing all emissions with $\tau > \tau_0$. This avoids double counting between the emissions contained in the QCD matrix elements and those generated by the parton showers. This algorithm has been tested against data, and overall the procedure seems to work very well [22].

A truly accurate next-to-leading order calculation would also incorporate loop diagrams. To obtain the matrix elements at NLO requires calculating the one-loop correction to the lowest order matrix element and combining it with the matrix element which describes the radiation of one additional parton. The difficulty in going to NLO is that both the virtual contributions at one loop and the real emission have infrared divergences, which only cancel when both diagrams are combined to calculate an infrared-safe observable [25,26], and this cancellation is difficult to encode numerically. MC@NLO [27] provides one solution (see also [28–34]). It uses the fact that the first splitting in the parton shower reproduces the IR divergence of the real QCD emission, and can thus be used to devise a subtraction from both the real and virtual diagrams that render both these contributions finite. This yields two separate matrix elements, which are both finite and can be used as starting conditions for a traditional parton shower. The initial results appear promising [35]. One problem is that MC@NLO works at the level of cross sections, not matrix elements, so it runs up against the possibility of having negative weights. It is also not clear how to generalize the procedure to higher orders.

III. JET DISTRIBUTIONS FROM SCET: SCHEMATICS

As we have seen in the previous section, the traditional Monte Carlo method uses splitting functions and Sudakov factors to generate a fully showered event. An event generator typically starts with an underlying hard process calculated using matrix elements of the full theory. The splitting functions then generate additional partons from these simple final states. The Sudakov factor, which is the probability of no-branching, is included, and it resums the large logarithms at leading order. The traditional Monte Carlo method uses splitting functions and Sudakov factors to generate a fully showered event. Both splitting functions and Sudakov factors can be derived in the limit of small transverse momentum, and parton showers are only correct in the limit where each successive branching has p_T much smaller that any previous branching: $Q \gg p_T^{(1)} \gg p_T^{(2)} \ldots$. Thus, only events with widely separated momentum scales can be described using parton-shower techniques. The occurrence of these widely separated scales makes it natural to reformulate the problem in the language of effective field theory. The appropriate effective theory for this problem is the soft collinear effective theory (SCET), which is designed to reproduce exactly long distance physics in the limit of collinear or soft radiation. SCET is a simplified version of QCD where only collinear and soft degrees of freedom are kept and all others have been integrated out. Any calculation using effective field theories requires three steps. First, one needs to match the effective theory onto the underlying theory. Matching determines coefficients in the effective theory such that at some short distance scale it exactly reproduces the underlying theory. This ensures that the effective theory below that scale contains the same information as the underlying theory. The scale for this matching calculation is typically chosen to coincide with the hard scale in the problem, for example, the center-of-mass energy of the collision. This ensures that the resulting short distance coefficients do not contain any large logarithms. Second, the effective theory is evolved to the lower scales arising in the process one wants to describe. This is achieved technically using renormalization group (RG) evolution, which sums logarithmic terms of the ratio of the low to the high scale. Finally, the matrix elements of the operators in the effective theory are calculated at the low scale.

As we will show in this paper, these steps naturally correspond to the ingredients in traditional parton showers mentioned above. The matching calculation encodes the hard underlying process which we want to study. The solution to the RG evolution gives rise to evolution kernels, which are equivalent to appropriate combinations of Sudakov factors. And the resulting matrix elements in SCET have the property that in the collinear limit their squares simplify to squares of simpler operators, multiplied by the splitting functions of QCD.

The first step is to match the full theory onto the effective theory at the hard scale Q. To match, we introduce operators in SCET and choose their coefficients such that the matrix elements in QCD and SCET are the same. The matching can be done perturbatively in α_s to any order. Once we have matched at the hard scale, we no longer need QCD. To be more specific, consider the process $e^+ e^- \rightarrow$ hadrons. In the standard model, this is mediated by a current

$$\mathcal{J} = \bar{q} \Gamma q, \qquad (11)$$

where $\Gamma = \gamma^\mu$ in the case of an intermediate photon or $\Gamma = g_V \gamma^\mu + g_A \gamma^\mu \gamma^5$ if the Z boson is included. The current has a nonvanishing matrix element in many final states, and we can compute $\langle \mathcal{J} | p_1 \cdots p_n \rangle \equiv \langle 0 | \mathcal{J} | p_1 \cdots p_n \rangle$ for any number of partons. In SCET, the process is mediated by operators which are constructed out of the fundamental objects of SCET: soft and collinear gluons, collinear quarks, and Wilson lines. Wilson lines are required to ensure gauge invariance of SCET, and each collinear field needs to be multiplied with Wilson lines in the appropriate SU(3) representation. For example, collinear fermions and collinear gluons always come in the combinations

$$\chi_n = W_n \xi_n, \qquad \mathcal{A}_n^\mu = \frac{1}{\bar{n} \cdot p} W_n [\bar{n} \cdot D, D^\mu] W_n^\dagger. \quad (12)$$

In the SCET literature $\mathcal{A}_\mu$ is commonly written as $B_\mu^\perp$. To reproduce the production of two collinear back-to-back partons one requires an operator in SCET which contains two collinear fields, one for each of the directions:

$$\mathcal{O}_2^{(n,\bar{n})} = \bar{\chi}_n \Gamma \chi_{\bar{n}}. \qquad (13)$$

Each operator comes with a set of labels, corresponding to the directions n_i of its collinear fields. We write

$$\mathcal{O}_j^{(n)} \sim \mathcal{O}_2^{(n_1, n_2)}, \mathcal{O}_3^{(n_1, n_2, n_3)}, \cdots, \qquad (14)$$

where n_j are the label momenta. The labels identify the degrees of freedom which cannot change—all the hard degrees of freedom which could have changed the collinear momentum in the full theory are integrated out of SCET. Note that there can be many operators with the same labels but different tensor structure (for example, the operators $\mathcal{O}_3$ and $\mathcal{O}_3^{(2)}$ we will define later on). For notational simplicity, we will often omit the labels (n_i) when there is no ambiguity.

The matching between QCD and SCET implies that we want to choose coefficients C_j for these operators such that the sum over all the operators reproduces the current of QCD

$$\mathcal{J} = C_2 \mathcal{O}_2 + C_3 \mathcal{O}_3 + C_4 \mathcal{O}_4 + \cdots. \qquad (15)$$

Since the Wilson coefficients C_j only encode short distance physics, they are independent of the choice of states used in

the calculation of matrix elements. So, to satisfy this equation, we can take matrix elements in convenient states, and build up the C_j systematically. First, we take matrix elements with two quarks in the final state, which gives the matching condition

$$\langle \mathcal{J} | q\bar{q} \rangle = C_2 \langle \mathcal{O}_2 | q\bar{q} \rangle, \qquad (16)$$

as no other higher-order operators have matrix elements in a 2-quark state. This allows us to determine C_2. Next, we take matrix elements with two quarks and one gluon

$$\langle \mathcal{J} | q\bar{q}g \rangle = C_2 \langle \mathcal{O}_2 | q\bar{q}g \rangle + C_3 \langle \mathcal{O}_3 | q\bar{q}g \rangle, \qquad (17)$$

and it allows us to determine C_3. The Wilson coefficients C_j with $j > 3$ are determined analogously. In order to correctly match QCD with up to m well-separated partons requires operators $\mathcal{O}_j$ with $n \le m$ in SCET. The next step is running. The matching determines the Wilson coefficients at the matching scale, $C_j(\mu = Q)$ and the running will allow us to obtain them at lower scales. The Wilson coefficients at these two scales are related by

$$C_n(\mu) = C_n(Q) \Pi_n(Q, \mu). \qquad (18)$$

The calculation of the evolution kernel Π_n is a straightforward application of the renormalization group, and it involves calculating the anomalous dimensions of the operators in SCET. Because the interactions in SCET are simpler than in QCD, the anomalous dimensions are fairly easy to compute. In fact, we will compute a closed form, algebraic expression, for the LL anomalous dimension of any $\mathcal{O}_j$.

The interactions in SCET allow for collinear gluons to be radiated off collinear quarks and gluons, or collinear gluons to split into two collinear quarks. However, since SCET only describes the collinear or soft limit of QCD, the transverse momentum between the resulting particles has to be small. How small depends on the renormalization scale at which the emission is calculated, and the requirement is typically $p_\perp \lesssim \mu$. As an example consider the matrix element of $\mathcal{O}_2$ in a three-parton final state with specific momenta $|q\bar{q}g\rangle$. Let p_T be the transverse momentum of the gluon with respect to a quark.[1] If the renormalization scale satisfies $\mu > p_T$, then gluon emission in SCET can give rise to a gluon in the final state, and a nonvanishing matrix element. If, however, $\mu < p_T$, then the SCET emission is not able to produce a gluon in the final state, and the matrix element of $\mathcal{O}_2$ vanishes. For theory to be continuous across p_T, matrix elements at the scale $\mu = p_T - \epsilon$ must be equal to matrix elements at $\mu = p_T + \epsilon$. More precisely, we require that

---

[1] Our notation is that $p_\perp$ is SCET notation for the perpendicular momentum label on a collinear field, while p_T refers to the transverse momentum between two four-vectors.

$$[C_2\langle\mathcal{O}_2\rangle + C_3\langle\mathcal{O}_3\rangle + \cdots]_{\mu=p_T+\epsilon}$$
$$= [C_2\langle\mathcal{O}_2\rangle + C_3\langle\mathcal{O}_3\rangle + \cdots]_{\mu=p_T-\epsilon}. \quad (19)$$

To compensate for the discontinuity of $\langle\mathcal{O}_2\rangle$ at $\mu = p_T$, we only need to change $C_3\langle\mathcal{O}_3\rangle$; all other matrix elements are continuous across the threshold. So we derive the matching condition

$$[C_2\langle\mathcal{O}_2\rangle]_{\mu=p_T+\epsilon} = [C_3^{(2)}\langle\mathcal{O}_3^{(2)}\rangle]_{\mu=p_T-\epsilon}. \quad (20)$$

We call this matching threshold matching and it is done wholly within SCET. Note that the operator $\mathcal{O}_3^{(2)}$ in Eq. (20) is different from the operator $\mathcal{O}_3$ arising in the hard matching at $\mu = Q$. To distinguish these operators we add a superscript, which labels the number of partons present at the hard matching scale. For simplicity, we omit the superscript for the operators matched at Q: $\mathcal{O}_j \equiv \mathcal{O}_j^{(j)}$. Let us apply these results and calculate the SCET expressions for a three jet final state, with the transverse momentum of the emitted gluon given by p_T. After matching QCD onto SCET at the hard scale $\mu = Q$ we find

$$\langle\text{SCET}\rangle_Q = C_2(Q)\langle\mathcal{O}_2\rangle + C_3(Q)\langle\mathcal{O}_3\rangle = \langle\text{QCD}\rangle. \quad (21)$$

Using the RG evolution, we can obtain this at a lower scale μ

$$\langle\text{SCET}\rangle_\mu = C_2(Q)\Pi_2(Q,\mu)\langle\mathcal{O}_2\rangle + C_3(Q)\Pi_3(Q,\mu)\langle\mathcal{O}_3\rangle. \quad (22)$$

Finally, at the $\mu = p_T$ we have to perform the threshold matching to obtain

$$\langle\text{SCET}\rangle_{p_T} = C_2(Q)\Pi_2(Q,p_T)\langle\mathcal{O}_3^{(2)}\rangle$$
$$+ C_3(Q)\Pi_3(Q,p_T)\langle\mathcal{O}_3\rangle. \quad (23)$$

This last step of matching is not required to obtain three jet final states, but we did include it here for completeness. To calculate a differential cross section, we need to square this matrix element and sum over final state spins and polarizations. Using the Feynman rules in SCET we will show later that emissions in SCET factorize. In particular,

$$|\langle\mathcal{O}_3^{(2)}|q\bar{q}g\rangle|^2 \approx |\langle\mathcal{O}_2|q\bar{q}\rangle|^2 P(p_T, z), \quad (24)$$

where $z = E_q/(E_g + E_q)$. The function $P(p_T, z)$ is equivalent to a splitting function of QCD, up to power corrections, in the collinear limit.

We can now show that SCET agrees with QCD for large p_T and the parton shower for small p_T. First, consider the limit $p_T \sim Q$. Then, $\Pi_n(Q, p_T) \sim 1$ up to higher-order corrections. So Eq. (23) reduces to Eq. (21) and we reproduce QCD. Next, take the limit $p_T \ll Q$. Then we are in the collinear limit, and so the matrix element of $\mathcal{O}_2$ is very similar to that of QCD. Thus, $\langle\mathcal{O}_3\rangle \approx 0$, since $\mathcal{O}_3$ is the difference between QCD and SCET. So $d\sigma \sim C_2(Q)\Pi_2^2\langle\mathcal{O}_3^{(2)}\rangle^2$. Now, the kernel Π_2, is equivalent to the

Sudakov factor, and as shown in Eq. (24), the matrix element reproduces a splitting function, therefore the SCET differential cross section in this limit reduces to the parton-shower result (8).

IV. REQUIRED CALCULATIONS IN SCET

In this section we present details of the SCET calculations required to implement the scheme from the previous section. As we have seen in the previous section, there are three steps in the SCET calculations required to obtain jet distributions. First, we need to calculate the matching from QCD to SCET at some hard scale $\mu \sim Q$. Second, the renormalization scale of the operators is lowered using the renormalization group evolution. Third, a threshold matching is required when the renormalization scale gets lowered past the transverse momentum of one of the partons in the final state. Each of these three steps will be addressed in its own subsection. We will try to keep results as general as possible, but sometimes it will be necessary to choose a particular example. In this section we assume that the reader is familiar with the basic idea of SCET. For a quick review of SCET we refer the reader to Appendix A and the original literature [2–5]. This is the most technical section of the paper, and for readers not interested in the details, we will briefly summarize the results obtained in this section. This will make it possible to skip this section and still be able to follow the rest of the paper.

The SCET results at $\mathcal{O}(\alpha_s)$ are as follows. The full QCD current is reproduced in the effective theory by operators $\mathcal{O}_n$, such that

$$\mathcal{J} = C_2\mathcal{O}_2 + C_3\mathcal{O}_3 + C_3^{(2)}\mathcal{O}_3^{(2)} + \cdots. \quad (25)$$

The operators are given by

$$\mathcal{O}_2 = \bar{\chi}_n\Gamma\chi_{\bar{n}}, \quad (26)$$

$$\mathcal{O}_3 = g_s\bar{\chi}_{n_q}\left[\mathcal{A}_{n_g}\frac{\slashed{n}_{\bar{q}}}{2}\frac{1}{n_{\bar{q}}\cdot\mathcal{P}^\dagger}\Gamma - \Gamma\frac{1}{n_q\cdot\mathcal{P}}\frac{\slashed{n}_q}{2}\mathcal{A}_{n_g}\right]\chi_{n_{\bar{q}}}, \quad (27)$$

$$\mathcal{O}_3^{(2)} = g_s\bar{\chi}_{n_q}\left[\mathcal{A}_{n_g}\frac{\slashed{\bar{n}}_{\bar{q}}}{2}\frac{1}{\bar{n}_{\bar{q}}\cdot\mathcal{P}^\dagger}\Gamma - \Gamma\frac{1}{\bar{n}_q\cdot\mathcal{P}}\frac{\slashed{\bar{n}}_q}{2}\mathcal{A}_{n_g}\right]\chi_{n_{\bar{q}}}, \quad (28)$$

and for the Wilson coefficients required to NLO we find

$$C_2(Q) = 1 - \frac{\alpha_s C_F}{4\pi}\left(8 - \frac{7\pi^2}{6} + 3\pi i\right), \quad (29)$$

$$C_3(Q) = 1, \quad (30)$$

$$C_3^{(2)}(p_T) = C_2(p_T). \quad (31)$$

The Wilson coefficients C_n satisfy the RG equation

$$\mu \frac{d}{d\mu} C_n(\mu) = \gamma_n(\mu) C_n(\mu). \tag{32}$$

The anomalous dimensions are

$$\gamma_2 = -\frac{\alpha_s}{\pi} \left[C_F \log\frac{-\mu^2}{Q^2} + C_F \frac{3}{2} \right], \tag{33}$$

$$\gamma_3 = -\frac{\alpha_s}{\pi} \left[C_F \left(\log\frac{-\mu^2}{(p_q + p_{\bar{q}})^2} + \frac{3}{2} \right) + \frac{C_A}{2} \right.$$
$$\left. \times \left(\log\frac{-\mu^2(p_q + p_{\bar{q}})^2}{(p_q + p_g)^2(p_{\bar{q}} + p_g)^2} + \frac{1}{6} \right) \right], \tag{34}$$

$$\gamma_n = -\frac{\alpha_s}{\pi} \left[\left(\frac{n_q}{2} C_F + \frac{n_g}{2} C_A \right) \log\frac{\mu^2}{Q^2} + B_n \right]. \tag{35}$$

The Wilson coefficients evolve through the kernels Π_n:

$$C_n(\mu_1) = C_n(\mu_2)\Pi_n(\mu_2, \mu_1). \tag{36}$$

For a general anomalous dimension

$$\gamma_n = -\frac{\alpha_s}{\pi} \left(\Gamma_n \log\frac{\mu^2}{Q^2} + B_n \right) \tag{37}$$

we can solve Π_n explicitly

$$\Pi_n(Q, \mu) = \exp\left\{ \frac{8\pi}{\beta_0^2 \alpha_s(Q)} \Gamma_n \left(\log\frac{\alpha_s(Q)}{\alpha_s(\mu)} + 1 - \frac{\alpha_s(Q)}{\alpha_s(\mu)} \right) \right.$$
$$\left. - \frac{2}{\beta_0} B_n \log\frac{\alpha_s(Q)}{\alpha_s(\mu)} \right\}$$
$$= 1 - \frac{\alpha_s(Q)}{4\pi} \left[\Gamma_n \log^2\frac{\mu^2}{Q^2} + 2B_n \log\frac{\mu^2}{Q^2} \right]$$
$$+ \cdots, \tag{38}$$

where

$$\alpha_s(\mu) = \frac{\alpha_s(Q)}{1 + \frac{\beta_0}{4\pi}\alpha_s(Q)\log\frac{\mu^2}{Q^2}}, \qquad \beta_0 = \frac{11}{3}C_A - \frac{2n_f}{3}. \tag{39}$$

Only the piece proportional to Γ_n is the leading-log resummation, the B_n resums a subset of next-to-leading logs.

A. Matching from QCD to SCET

The first step is matching from QCD to SCET. As discussed in Sec. III, the matching condition is

$$\mathcal{J} = C_2\mathcal{O}_2 + C_3\mathcal{O}_3 + C_4\mathcal{O}_4 + \cdots, \tag{40}$$

and we want to choose Wilson coefficients in the effective theory such that QCD is reproduced at the scale Q to a given order in perturbation theory. QCD matrix elements with up to n well-separated partons appear at $\mathcal{O}(g_s^{n-2})$ in

perturbation theory. In order to correctly reproduce these matrix elements, we require operators in SCET with up to n collinear fields. In the remainder of this section, we will explicitly perform the matching onto operators $\mathcal{O}_2$ and $\mathcal{O}_3$, and comment on how to extend these calculations to operators with four or more collinear fields. As discussed above, each operator $\mathcal{O}_j$ depends on j labels for the directions of the j collinear fields. For each set of labels a different Wilson coefficient exists, so that in principle each product of operator and Wilson coefficient in Eq. (40) represents an infinite sum over the various labels. We will carefully treat the label dependence in the two-jet matching, but will then neglect the label dependence in the further discussions.

1. Matching onto $\mathcal{O}_2$ at tree level

The first step is to ensure that matrix elements with two quarks are correctly reproduced. Since the operators $\mathcal{O}_j$ with $j > 2$ have at least 3 collinear fields, they do not contribute to these matrix elements. Thus we need to choose Wilson coefficients $C_2^{(n)}$ so that

$$\langle \mathcal{J}|q\bar{q}\rangle = \sum_{n_i} C_2^{n_1 n_2} \langle \mathcal{O}_2^{(n_1, n_2)}|q\bar{q}\rangle, \tag{41}$$

where

$$\mathcal{O}_2^{(n_1, n_2)} = \bar{\chi}_{n_1} \Gamma \chi_{n_2} \tag{42}$$

is a general basis of operators with 2 collinear fermion fields. To evaluate matrix elements on the right-hand side of (41), we need to know how jets χ_n act on quark states $|q\rangle$. The simplest prescription is

$$\chi_n|q\rangle = \delta_{n^\mu, n_q^\mu}, \tag{43}$$

where $n_q^\mu = p_q^\mu/E_q$. If $\mathcal{J}$ produces two quarks, they must be back-to-back in the center-of-mass frame. So with this prescription, only the operators with $n_2 = \bar{n}_1$ get a nonzero coefficient. With these conventions, the matrix elements of the operator $\mathcal{O}_2$ is identical to the matrix element of the QCD current $\mathcal{J}$ and we thus obtain

$$C_2^{n,\bar{n}} = 1, \qquad C_2^{n_1, n_2} = 0, \qquad n_1 \neq \bar{n}_2. \tag{44}$$

SCET fields also have labels corresponding to their $p_\perp$ momenta, but we choose to turn off any operator with $p_\perp \neq 0$. Other choices for collinear fields acting on quark states are possible, and in fact (43) is by itself ambiguous. We can always write χ_n as a jet in a different direction n' using (A7)

$$\chi_n = \frac{\not{n}\not{\bar{n}}}{4} \left[1 + \frac{\not{p}_\perp}{\bar{n}' \cdot p} \frac{\not{\bar{n}}'}{2} \right] \chi_{n'}, \tag{45}$$

where $p_\perp$ is transverse to n'. Thus it would seem that $\chi_n|q\rangle \neq 0$ even if q is not aligned with n. This ambiguity is resolved at higher order. Note that $n \cdot n' \sim p_\perp^2$, thus as

long as $n \cdot n' \ll 1$ the two fields are equivalent up to power corrections. This implies that any operator $\bar{\chi}_{n_1} \Gamma \chi_{n_2}$ with $n_1 \cdot n_2 \ll 1$ could be used as the operator $\mathcal{O}_2$. Of course, in order to determine the matrix element of the operator $\mathcal{O}_2$ requires knowledge of how a SCET field with a given direction n creates or annihilates a final state with momentum in a direction n'. Any choice other than Eq. (43) will make the required calculations more difficult, so for simplicity we will stick to (43) for the rest of this paper.

2. Matching onto $\mathcal{O}_3$ at tree level

Now that we have determined the matching onto the operator $\mathcal{O}_2$ we can proceed to match with 3-parton final states. The matching condition reads

$$\langle \mathcal{J} | q\bar{q}g \rangle = C_2 \langle \mathcal{O}_2 | q\bar{q}g \rangle + C_3 \langle \mathcal{O}_3 | q\bar{q}g \rangle. \quad (46)$$

The left-hand side is given by the matrix elements for real emission in QCD from the quark and the antiquark leg

$$\langle \mathcal{J} | q\bar{q}g \rangle^q = g_s \bar{\psi}_q \frac{\mathcal{A}(\not{p}_q + \not{p}_g)}{(p_q + p_g)^2} \Gamma \psi_{\bar{q}},$$

$$\langle \mathcal{J} | q\bar{q}g \rangle^{\bar{q}} = -g_s \bar{\psi}_q \Gamma \frac{(\not{p}_{\bar{q}} + \not{p}_g)\mathcal{A}}{(p_{\bar{q}} + p_g)^2} \psi_{\bar{q}}. \quad (47)$$

For the right-hand side, the operator $\mathcal{O}_2$ and its Wilson coefficient were determined in the previous section, but we need to evaluate the three-parton matrix element for $\mathcal{O}_2$. In principle, the additional gluon can be either collinear or soft. We will first choose the gluon to be collinear and later check that the resulting matching condition is satisfied in the soft limit as well. The collinear emissions in SCET can come out of either a vertex from the Lagrangian or from a Wilson line. The matrix elements are extracted from the interaction vertices, and simplify with the equations of motion $\not{\bar{n}}\xi_{\bar{n}} = \bar{\xi}_n \not{n} = 0$.

$$\langle \mathcal{O}_2 | q\bar{q}g \rangle^{L_q} = g_s \frac{\bar{n} \cdot (p_q + p_g)}{(p_q + p_g)^2} \bar{\xi}_n A_\mu \left[n^\mu + \frac{\not{p}_q^\perp \gamma_\perp^\mu}{\bar{n} \cdot p_q} + \frac{\gamma_\perp^\mu(\not{p}_q^\perp + \not{p}_g^\perp)}{\bar{n} \cdot (p_q + p_g)} - \frac{\not{p}_q^\perp(\not{p}_q^\perp + \not{p}_g^\perp)}{\bar{n} \cdot p_q \bar{n} \cdot (p_q + p_g)} \bar{n}^\mu \right] \Gamma \xi_{\bar{n}},$$

$$\langle \mathcal{O}_2 | q\bar{q}g \rangle^{L_{\bar{q}}} = -g_s \frac{n \cdot (p_{\bar{q}} + p_g)}{(p_{\bar{q}} + p_g)^2} \bar{\xi}_n \Gamma \left[\bar{n}^\mu + \frac{\gamma_\perp^\mu \not{p}_{\bar{q}}^\perp}{n \cdot p_{\bar{q}}} + \frac{(\not{p}_{\bar{q}}^\perp + \not{p}_g^\perp)\gamma_\perp^\mu}{n \cdot (p_{\bar{q}} + p_g)} - \frac{(\not{p}_{\bar{q}}^\perp + \not{p}_g^\perp)\not{p}_{\bar{q}}^\perp}{n \cdot (p_{\bar{q}} + p_g) n \cdot p_{\bar{q}}} n^\mu \right] A_\mu \xi_{\bar{n}}, \quad (48)$$

$$\langle \mathcal{O}_2 | q\bar{q}g \rangle^{W_q} = g_s \bar{\xi}_n \frac{\bar{n} \cdot A}{\bar{n} \cdot p_g} \Gamma \xi_{\bar{n}}, \qquad \langle \mathcal{O}_2 | q\bar{q}g \rangle^{W_{\bar{q}}} = -g_s \bar{\xi}_n \Gamma \frac{n \cdot A}{n \cdot p_g} \xi_{\bar{n}}.$$

As the SCET Lagrangian is constructed to be gauge invariant, the matrix elements should satisfy a Ward identity. It is a straightforward check to see that $\langle \mathcal{O}_2 | q\bar{q}g \rangle^W + \langle \mathcal{O}_2 | q\bar{q}g \rangle^L$ vanishes when $A^\mu = p_g^\mu$. This holds separately for the quark and antiquark emissions, as it must since SCET is invariant under gauge transformations of the collinear fields in each direction separately. There are several issues that have to be resolved before we can use the above results to determine the matching of the operator $\mathcal{O}_3$. First, note that the collinear emission from a Wilson line gives a divergence if the large label momentum ($\bar{n} \cdot p_g$ for $\langle \mathcal{O}_2 \rangle^{W_q}$ and $n \cdot p_g$ for $\langle \mathcal{O}_2 \rangle^{W_{\bar{q}}}$) becomes small. In SCET, the collinear phase space integration involves summing over the large momentum labels, as well as integrating over the residual part of the momentum. However, in the sum over collinear momenta the value $\bar{n} \cdot p = 0$ and $p^\perp = 0$ has to be omitted [36]. Thus, the phase space integration will never reach a value for the label momentum such that the unphysical divergence is realized. However, keeping track of the condition $\bar{n} \cdot p \neq 0$ in the phase space integration can be difficult, and we therefore propose a scheme which will allow us to integrate the phase space naively, without having to worry about small label momenta. In this scheme one neglects the emissions from the collinear Wilson lines all together, and ensures gauge invariance by summing over only transverse polarizations when squaring the resulting matrix elements. By neglecting the
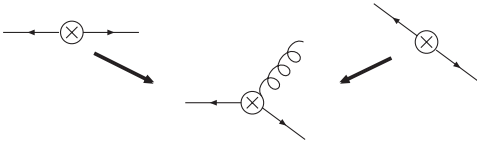
$\langle \mathcal{O}_2 \rangle^W$ contributions, we subtract the divergences at small $\bar{n} \cdot p$. Any appropriate prescription will modify the effective theory only at short distances, and therefore differences in prescription can be absorbed by appropriately adjusting the Wilson coefficients in the matching condition. In practice, however, we have to evaluate matrix elements at finite momenta, which are neither exactly at the hard scale where the matching is done, nor in the strict collinear limit, where the different prescriptions coincide. Therefore the physical results may differ. However, these differences are beyond leading order in the SCET expansion, i.e. they are power corrections.

The second issue is that emissions in SCET cannot change the directions of the fermions. Since the operators $\mathcal{O}_2$ that were matched on in the two-jet matching have the two fermions in back-to-back directions, the matrix element of $\mathcal{O}_2$ can only give rise to final state with back-to-back fermions. But if momentum is to be conserved when we include the gluon, the directions of the quark and antiquark momenta can never satisfy $n_q = \bar{n}_{\bar{q}}$ exactly. This implies that in order to insist on (43), we need to change the direction of at least one of $\bar{\xi}_n$ or $\xi_{\bar{n}}$ using (45), otherwise we could never get a nonvanishing matrix element with three partons in different directions. There are again various possibilities to deal with this, and all of them will lead to the same results up to power corrections. The choice we will adopt here is that directions of collinear

fields which are not involved in the emission do not change. Then we rotate the emitting field into the direction of its final state. In other words, we use

$$\bar{\xi}_n \Omega[\Gamma \xi_{\bar{n}}] \rightarrow \bar{\xi}_{n_q} \frac{\not{n}_{\bar{q}} \bar{\not{n}}_{\bar{q}}}{4} \Omega[\Gamma \xi_{n_q}],$$

$$[\bar{\xi}_n \Gamma] \Omega \xi_{\bar{n}} \rightarrow [\bar{\xi}_{n_q} \Gamma] \Omega \frac{\bar{\not{n}}_q \not{n}_q}{4} \xi_{n_{\bar{q}}}, \tag{49}$$

where Ω is some arbitrary operator. This equation shows how to replace a fermion in SCET with a fermion in QCD, which is necessary to compare matrix elements in the same external states. We now see that two *different* operators $\mathcal{O}_2^{(n_{\bar{q}} \bar{n}_q)}$ and $\mathcal{O}_2^{(n_q \bar{n}_q)}$ contribute to the same final state. Pictorially,

The first will turns $\mathcal{O}_2$ into $\mathcal{O}_3^{(3)}$ when the quark emits, and the second when the antiquark emits. We want to emphasize again that this is just a convention, and equivalent to any other convention up to power corrections.

The transverse momenta are measured with respect to the directions n and $\bar{n}$. This implies that when the quark emits, $p_q^\perp + p_g^\perp = 0$ and when the antiquark emits, $p_{\bar{q}}^\perp + p_g^\perp = 0$. Using these results together with (49), the quark emission and antiquark emission contributions to the matrix element of $\mathcal{O}_2$ can be simplified to

$$\langle \mathcal{O}_2 | q\bar{q}g \rangle^{L_q} = g_s \frac{n_{\bar{q}} \cdot (p_q + p_g)}{(p_q + p_g)^2} \bar{\xi}_{n_q} \not{A} \frac{\bar{\not{n}}_{\bar{q}}}{2} \Gamma \xi_{n_{\bar{q}}},$$

$$\langle \mathcal{O}_2 | q\bar{q}g \rangle^{L_{\bar{q}}} = -g_s \frac{n_q \cdot (p_{\bar{q}} + p_g)}{(p_{\bar{q}} + p_g)^2} \bar{\xi}_{n_q} \Gamma \frac{\bar{\not{n}}_q}{2} \not{A} \xi_{n_{\bar{q}}}. \tag{50}$$

Using the results of the SCET matrix elements given in Eq. (50) and the QCD matrix elements given in Eq. (47), their difference reduces to the simple form [1]

$$\langle \mathcal{J} | q\bar{q}g \rangle^q - \langle \mathcal{O}_2 | q\bar{q}g \rangle^{L_q}$$

$$= g_s \frac{\bar{n}_{\bar{q}} \cdot (p_q + p_g)}{(p_q + p_g)^2} \bar{\xi}_{n_q} \not{A} \frac{\bar{\not{n}}_{\bar{q}}}{2} \Gamma \xi_{n_{\bar{q}}},$$

$$\langle \mathcal{J} | q\bar{q}g \rangle^{\bar{q}} - \langle \mathcal{O}_2 | q\bar{q}g \rangle^{L_{\bar{q}}}$$

$$= -g_s \frac{\bar{n}_q \cdot (p_{\bar{q}} + p_g)}{(p_{\bar{q}} + p_g)^2} \bar{\xi}_{n_q} \Gamma \frac{\not{n}_q}{2} \not{A} \xi_{n_{\bar{q}}}. \tag{51}$$

The final step in the matching is to choose a basis for the 3-jet operators $\mathcal{O}_3^{(n)}$. The standard convention is to have $C_3 = 1$ at tree level, so we take $\mathcal{O}_3 = \mathcal{J} - \mathcal{O}_2$. Thus, we arrive at

$$\mathcal{O}_3 = g_s \bar{\chi}_{n_q} \left(\mathcal{A}_{n_g} \frac{\not{n}_{\bar{q}}}{2} \frac{1}{n_{\bar{q}} \cdot \mathcal{P}^\dagger} \Gamma - \Gamma \frac{1}{n_q \cdot \mathcal{P}} \frac{\not{n}_q}{2} \mathcal{A}_{n_g} \right) \chi_{n_{\bar{q}}},$$

$$C_3 = 1, \tag{52}$$

where $\mathcal{A}_n^\mu$ was defined in Eq. (12). Note that $\mathcal{O}_3$ is the difference between the QCD and SCET emissions. Since the operator $\mathcal{O}_2$, together with the SCET emission of an additional gluon describes the infrared physics of QCD, the operator $\mathcal{O}_3$ only has contributions for large values of the transverse momentum. If the gluon is soft instead of collinear, there are two emission diagrams in SCET. The matrix elements are

$$\langle \mathcal{O}_2 | q\bar{q}g \rangle^{S_q} = g_s \bar{\xi}_n \frac{n \cdot A}{n \cdot p_g} \Gamma \xi_{\bar{n}},$$

$$\langle \mathcal{O}_2 | q\bar{q}g \rangle^{S_{\bar{q}}} = -g_s \bar{\xi}_n \Gamma \frac{\bar{n} \cdot A}{\bar{n} \cdot p_g} \xi_{\bar{n}}. \tag{53}$$

This can be compared with the collinear results given our convention of dealing with label momenta going to zero. In that scheme we only keep the matrix elements $\langle \mathcal{O} \rangle^L$ and sum only over transverse polarizations of the gluons. Taking the soft limit of $\langle \mathcal{O}_2 | q\bar{q}g \rangle$ (by taking $p_g \ll \bar{n} \cdot p_q, n \cdot p_{\bar{q}}$) we find

$$\langle \mathcal{O}_2 | q\bar{q}g \rangle^{L_q} \rightarrow g_s \bar{\xi}_n \frac{n \cdot A}{n \cdot p_g} \Gamma \xi_{\bar{n}},$$

$$\langle \mathcal{O}_2 | q\bar{q}g \rangle^{L_{\bar{q}}} \rightarrow -g_s \bar{\xi}_n \Gamma \frac{\bar{n} \cdot A}{\bar{n} \cdot p_g} \xi_{\bar{n}}. \tag{54}$$

Thus, the soft limit of the collinear Lagrangian emission is identical to the soft gluon emission. However, care has to be taken about the second part of the convention, namely, the fact that we only sum over transverse polarizations. Since for gauge invariant amplitudes the longitudinal polarizations do not contribute to physical processes, the soft gauge invariance of SCET is enough to ensure that the sum over transverse polarizations is equivalent to the sum over all polarizations. SCET is by construction gauge invariant, but one can also see the invariance trivially from Eq. (54). Replacing $A^\mu \rightarrow p_g^\mu$, the two contributions are equal and opposite in sign and thus cancel. Thus, the amplitude satisfies the Ward identity and is gauge invariant. With these two observations it is obvious that the collinear emission reproduces the soft emission properly. In summary, we have chosen the conventions

  (i) All fields appearing in operators have labels for collinear momenta only; in our basis, all $p_\perp$ momentum components are zero.

 (ii) Emissions are calculated with the collinear emission from the SCET Lagrangian only. Wilson line emission and soft emission are discarded.

(iii) To maintain gauge invariance, we include only transverse polarizations of the gluons.

(iv) Fermions in SCET are rotated to a direction aligned

with their 4-momentum before matrix elements are taken, i.e. $\xi_n \to \frac{\not{n}\not{\bar{n}}}{4} \xi_{n_q}$, where $n_q^\mu = \frac{1}{E_q} q^\mu$ for massless fields.

All other conventions are equivalent up to power corrections.

3. Matching onto $\mathcal{O}_4$ at tree level

We can outline the calculation for matching 4-jet operators $\mathcal{O}_4$. These will make up for the difference between what SCET predicts when we have used only 3-parton QCD results, and the true 4-parton QCD prediction. Starting from $q\bar{q}$, a 4-parton state can be either $qg g\bar{q}$ or $q\bar{q}q\bar{q}$. We need to solve

$$\langle \mathcal{J}|4\rangle = \sum_{(n)} \mathrm{C}_2^{(n)} \langle \mathcal{O}_2^{(n)}|4\rangle + \mathrm{C}_3^{(n)} \langle \mathcal{O}_3^{(n)}|4\rangle + \mathrm{C}_4^{(n)} \langle \mathcal{O}_4^{(n)}|4\rangle. \tag{55}$$

Let us take the $|q\bar{q}q\bar{q}\rangle$ state as an example. Then there are two QCD diagrams which contribute

$$\langle \mathcal{J}|q\bar{q}q\bar{q}\rangle = \quad + \quad \tag{56}$$

On the SCET side, the $\mathcal{O}_2$'s can contribute

$$\langle \mathcal{O}_2|q\bar{q}q\bar{q}\rangle = \quad + \quad \tag{57}$$

as well as $\mathcal{O}_3$

$$\langle \mathcal{O}_3|q\bar{q}q\bar{q}\rangle = \quad \tag{58}$$

and of course $\mathcal{O}_4$:

$$\langle \mathcal{O}_4|q\bar{q}q\bar{q}\rangle = \quad \tag{59}$$

Using the results for $\mathcal{O}_2$ and $\mathcal{O}_3$ obtained previously, we can determine C_4 and $\mathcal{O}_4$. In a similar way, the tree-level matching for n jets can be worked out. Note that since we have already set the conventions for evaluating matrix elements, there is no additional ambiguity when we match to operators with 4 or more collinear fields.

4. 2-jet matching at NLO

So far, we have performed the matching calculations at tree level, and the normalization of the operators was chosen such that all Wilson coefficients are unity. In this subsection, we will determine the Wilson coefficient C_2 at $\mathcal{O}(\alpha_s)$, which will be required to describe jet distributions at NLO. The matching condition is still given by Eq. (41),

but the matrix elements need now be evaluated at one loop. Loop diagrams are in general both IR and UV divergent, and we regulate IR divergences by adding quarks and gluon virtualities p_j^2, while using dimensional regularization with $d = 4 - 2\epsilon$ for the UV divergences. As always, the UV divergences are removed with counterterms, and the IR divergences cancel in the matching. For renormalization we will use modified minimal subtraction, with μ as the $\overline{\mathrm{MS}}$ renormalization scale.

The one-loop QCD vertex correction [37] is

$$\mathcal{A}_{\mathcal{J}}^{(2)} = \quad$$
$$= -\frac{\alpha_s C_F}{4\pi} \left[-\frac{1}{\epsilon} + 2\log\frac{p_q^2}{Q^2}\log\frac{p_{\bar{q}}^2}{Q^2} + 2\log\frac{p_q^2 p_{\bar{q}}^2}{Q^4} \right.$$
$$\left. + \log\frac{-Q^2}{\mu^2} + \frac{2\pi^2}{3} \right]. \tag{60}$$

We draw the photon explicitly, because this graph depends on choosing $\Gamma = \gamma^\mu$.

The SCET diagrams involve collinear gluons [2]:

$$= -\frac{\alpha_s C_F}{4\pi} \left[-\frac{2}{\epsilon^2} - \frac{2}{\epsilon} + \frac{2}{\epsilon}\log\frac{-p_q^2}{\mu^2} \right.$$
$$\left. - \log^2\frac{-p_q^2}{\mu^2} + 2\log\frac{-p_q^2}{\mu^2} - 4 + \frac{\pi^2}{6} \right] \tag{61}$$

$$= -\frac{\alpha_s C_F}{4\pi} \left[-\frac{2}{\epsilon^2} - \frac{2}{\epsilon} + \frac{2}{\epsilon}\log\frac{-p_{\bar{q}}^2}{\mu^2} \right.$$
$$\left. - \log^2\frac{-p_{\bar{q}}^2}{\mu^2} + 2\log\frac{-p_{\bar{q}}^2}{\mu^2} - 4 + \frac{\pi^2}{6} \right] \tag{62}$$

and soft gluons:

$$= -\frac{\alpha_s C_F}{4\pi} \left[\frac{2}{\epsilon^2} - \frac{2}{\epsilon}\log\frac{-p_q^2 p_{\bar{q}}^2}{\mu^2 Q^2} \right.$$
$$\left. + \log^2\frac{-p_{\bar{q}}^2 p_q^2}{\mu^2 Q^2} + \frac{\pi^2}{2} \right] \tag{63}$$

We have not assumed the quarks are back to back in computing any of these diagrams; $n_q \cdot n_{\bar{q}}$ appears in the final result only through Q^2. The SCET graphs do not depend on the choice of Γ. The sum of the three SCET diagrams gives

$$\mathcal{A}_{\mathcal{O}}^{(2)} = -\frac{\alpha_s C_F}{4\pi} \left[-\frac{2}{\epsilon^2} - \frac{4}{\epsilon} + \frac{2}{\epsilon}\log\frac{-Q^2}{\mu^2} \right.$$
$$+ 2\log\frac{p_q^2}{Q^2}\log\frac{p_{\bar{q}}^2}{Q^2} + 2\log\frac{p_q^2}{Q^2} + 2\log\frac{p_{\bar{q}}^2}{Q^2}$$
$$\left. - \log^2\frac{-Q^2}{\mu^2} + 4\log\frac{-Q^2}{\mu^2} - 8 + \frac{5\pi^2}{6} \right]. \tag{64}$$

Note how the $\frac{1}{\epsilon}\log p_j^2$ pieces, which are UV and IR divergent, drop out of the sum. This is a consistency check, as such divergences cannot be removed with counterterms.

We can see explicitly that the entire dependence on the IR regulators p_q^2 and $p_{\bar{q}}^2$ is the same in $\mathcal{A}_{\mathcal{J}}^{(2)}$ and $\mathcal{A}_{\mathcal{O}}^{(2)}$, as expected. Taking the difference between the QCD and the SCET amplitude we find

$$
\mathcal{A}_{\mathcal{J}}^{(2)} - \mathcal{A}_{\mathcal{O}}^{(2)} = -\frac{\alpha_s C_F}{4\pi}\left[\frac{2}{\epsilon^2} + \frac{3}{\epsilon} - \frac{2}{\epsilon}\log\frac{-Q^2}{\mu^2}\right.
$$
$$
\left. + \log^2\frac{-Q^2}{\mu^2} - 3\log\frac{-Q^2}{\mu^2} + 8 - \frac{\pi^2}{6}\right].
$$
(65)

The $1/\epsilon$ UV divergences are canceled by counterterm contributions, and matching at $\mu = Q$, we get

$$
\mathrm{C}_2(Q) = 1 - \frac{\alpha_s C_F}{4\pi}\left[8 - \frac{7\pi^2}{6} + 3\pi i\right].
$$
(66)

To determine the counterterms of the operator $\mathcal{O}_2$ we need the wave function renormalizations as well. For the matching, these were not required, since they are exactly the same in QCD an in SCET [3]. One finds
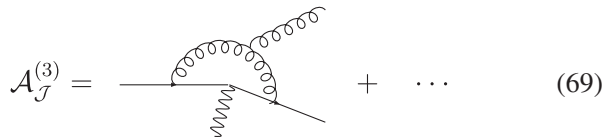
$$
Z_\xi = 1 - \frac{\alpha_s C_F}{4\pi}\left[\frac{1}{\epsilon} - \log\frac{-p^2}{\mu^2} + 1\right].
$$
(67)

Combining this with the vertex diagram gives the result that the UV divergences in the full theory cancel, as is expected for a conserved current. We find that the renormalization constant in QCD is just 1, while in SCET

$$
Z_2 = 1 + \frac{\alpha_s(\mu)C_F}{4\pi}\left[\frac{2}{\epsilon^2} + \frac{2}{\epsilon}\log\frac{-\mu^2}{Q^2} + \frac{3}{\epsilon}\right].
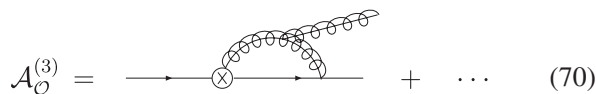$$
(68)

5. 3-jet matching at NLO

We can also match QCD onto 3-jet operators at NLO. We will not perform the calculation here, but merely outline what is required and make some qualitative comments. The 3-jet NLO matching involves calculating the difference between QCD diagrams such as

$$
\mathcal{A}_{\mathcal{J}}^{(3)} = \qquad\qquad + \quad \cdots
$$
(69)

and SCET diagrams, such as

$$
\mathcal{A}_{\mathcal{O}}^{(3)} = \qquad\qquad + \quad \cdots
$$
(70)

There are also contributions from the same diagrams required for γ_3, below. As for the 2-jet operators at NLO, the

QCD calculation and the SCET calculation are separately divergent, but the divergences all cancel in the difference.

Note, however, that in this case, there is no reason to expect the structure of the operator which results to be the same as $\mathcal{O}_3$. So we must add a new operator to the theory whose Wilson coefficient starts at $\mathcal{O}(\alpha_s)$. This operator, when squared (or interfered with $\mathcal{O}_3$), will produce a differential distribution for 3-jet events which has a different shape than the tree-level 3-parton distribution. In this way, all the shape changes from loop corrections in QCD can be reproduced in SCET. We will return to this discussion in Sec. V C.

B. Running

While the operators in SCET reproduce the long distance physics of QCD, their short distance behavior is completely different. In particular, the operator $\mathcal{O}_2$ is divergent in the UV, while the full QCD current $\bar{q}\gamma^\mu q$ is not. The matching performed in the previous section ensured that at some particular scale the matrix elements in SCET reproduce the matrix elements of QCD exactly at a given order in perturbation theory. All the difference between the short distance behavior of QCD and SCET above the matching scale $\mu = Q$ is absorbed in the precise numerical value of the Wilson coefficients $\mathrm{C}_n(Q)$. If the matching would have been performed at a different scale, the difference between QCD and SCET matrix elements would have been different, since the amount of short distance physics that has to be accounted for is different in that case. Thus, the Wilson coefficients C_n must depend on the value of the matching scale μ. Since μ is just a renormalization scale, it has no observable physical effect and our final answer should be independent of this scale. This implies that the matrix elements in the effective theory should satisfy a RG equation

$$
\mu\frac{d}{d\mu}[\mathrm{C}_2(\mu)\mathcal{O}_2(\mu) + \mathrm{C}_3(\mu)\mathcal{O}_3(\mu) + \ldots
$$
$$
+ \mathrm{C}_n(\mu)\mathcal{O}_n(\mu)] = 0.
$$
(71)

Since each operator $\mathcal{O}_n$ contains a different number of labeled collinear fields and interactions in the effective theory cannot change this number, each contribution has to separately satisfy the RG equation[2]

$$
\mu\frac{d}{d\mu}[\mathrm{C}_n(\mu)\mathcal{O}_n(\mu)] = 0.
$$
(72)

The μ dependence enters the operator $\mathcal{O}_n$ only through its renormalization constant Z_n. The anomalous dimension of an operator is defined as

---

[2]Beyond leading order, there may be mixing among operators. In this case the anomalous dimensions would be matrices, but we stick to the case without mixing for simplicity.

$$\gamma_n \equiv \frac{1}{Z_n(\mu)} \mu \frac{d}{d\mu} Z_n(\mu). \qquad (73)$$

This allows us to write the RG equation in its final form

$$\mu \frac{d}{d\mu} C_n(\mu) = \gamma_n(\mu) C_n(\mu). \qquad (74)$$

This differential equation can be written as an integral equation

$$\Pi_n(\mu_2, \mu_1) \equiv \frac{C_n(\mu_1)}{C_n(\mu_2)} = \exp\left[-\int_{\mu_1}^{\mu_2} \frac{d\mu}{\mu} \gamma_n(\mu) \right]. \qquad (75)$$

We call Π_n the RG evolution kernel. It determines the change of a Wilson coefficient C_n as the scale changes. Thus, if we have calculated the Wilson coefficients C_n at one scale, we can use this kernel to obtain its value at any other scale. The anomalous dimensions will have the form

$$\gamma_n = -\left[\frac{\alpha_s(\mu)}{\pi} \Gamma_n^{(1)} + \left(\frac{\alpha_s(\mu)}{\pi}\right)^2 \Gamma_n^{(2)} + \dots \right] \log\frac{\mu^2}{Q^2}$$
$$- \left[\frac{\alpha_s(\mu)}{\pi} B_n^{(1)} + \left(\frac{\alpha_s(\mu)}{\pi}\right)^2 B_n^{(2)} + \dots \right]. \qquad (76)$$

The first term in brackets is often called the cusp anomalous dimension. It multiplies an explicit, linear dependence on $\log\mu$. This term arises because of the double $1/\epsilon^2$ poles in the renormalization constants Z_n, which in turn can be traced back to the fact that full QCD has overlapping soft and collinear divergences. Such a term in the anomalous dimension is not problematic if no higher powers of logarithms appear, because it can be resumed. And in fact, it has been shown that at any order in perturbation theory the anomalous dimension contains at most a linear dependence on such a logarithm [37].

As a practical matter, it is helpful to have an explicit form for the evolution kernel (75). At leading order in α_s

$$\gamma_n(\mu) = -\frac{\alpha_s(\mu)}{\pi} \left(\Gamma_n \log\frac{\mu^2}{Q^2} + B_n \right), \qquad (77)$$

where Γ_n and B_n do not depend on μ. The integral over μ can then be performed explicitly, and we find

$$\Pi_n(Q, \mu) = \exp\left\{ \frac{8\pi}{\beta_0^2 \alpha_s(Q)} \Gamma_n \left(\log\frac{\alpha_s(Q)}{\alpha_s(\mu)} + 1 - \frac{\alpha_s(Q)}{\alpha_s(\mu)} \right) \right.$$
$$\left. - \frac{2}{\beta_0} B_n \log\frac{\alpha_s(Q)}{\alpha_s(\mu)} \right\}. \qquad (78)$$

From the integrated expression, it is easy to see that the B_n piece is subleading to Γ_n; the latter has an additional log enhancement. Moreover, when we change the reference scale μ_R then the coefficient of $\log\alpha_2/\alpha_1$ will shift, showing that there are additional contributions at NLL of the same order as B_n. Thus, only the cusp anomalous dimension is required for leading-log resummation.

We will now determine the anomalous dimensions γ_2 and γ_3 at $\mathcal{O}(\alpha_2)$ and the cusp anomalous dimension for γ_n.

1. Calculating γ_2

The counterterm of the operator $\mathcal{O}_2$ was already obtained in the previous section as a byproduct of the calculation of C_2 at one loop. We found in Eq. (68)

$$\gamma_2(\mu) = -\frac{\alpha_s(\mu) C_F}{\pi} \left[\log\frac{-\mu^2}{Q^2} + \frac{3}{2} \right]. \qquad (79)$$
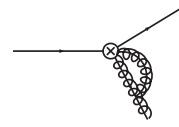
This has the form (76) as expected. We can then plug into (78) with

$$\Gamma_2 = C_F \quad \text{and} \quad B_2 = C_F\left(\frac{3}{2} + \pi i\right). \qquad (80)$$

Note that the anomalous dimension is complex. This is due to a physical effect. Because degrees of freedom have been integrated out, some fields which would go on shell when we cut a QCD diagram are no longer around. But for the theories to be the same, the imaginary parts of the cuts must be made up for somewhere else, and so they show up in the anomalous dimension.
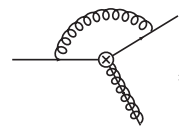
2. Calculating γ_3

To get the anomalous dimension for $\mathcal{O}_3$, we need to calculate its renormalization constant. We will again regulate the UV by dimensional regularization, and add a virtuality to all external particles to regulate the collinear and soft IR physics. The collinear graphs involving the fermions are the same as for $\mathcal{O}_2$, and given in (61) and (62). The collinear graph involving the gluon is [38]
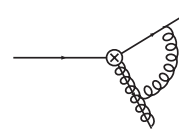

$$= -\frac{\alpha_s C_A}{4\pi} \left[-\frac{2}{\epsilon^2} - \frac{1}{\epsilon} + \frac{2}{\epsilon} \log\frac{-p_g^2}{\mu^2} \right.$$
$$\left. - \log^2\frac{-p_g^2}{\mu^2} + \log\frac{-p_g^2}{\mu^2} - 2 + \frac{\pi^2}{6} \right]. \qquad (81)$$

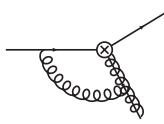The soft graph across the fermions is the same as (63), up to group theory factors:

$$= -\frac{\alpha_s}{4\pi}\left(\frac{1}{2}C_A - C_F\right)\left[-\frac{2}{\epsilon^2} + \frac{2}{\epsilon}\log\frac{-p_q^2 p_{\bar{q}}^2}{\mu^2(p_q + p_{\bar{q}})^2} \right.$$
$$\left. - \log^2\frac{-p_q^2 p_{\bar{q}}^2}{\mu^2(p_q + p_{\bar{q}})^2} - \frac{\pi^2}{2} \right] \qquad (82)$$

The soft graph between gluons and quarks are

$$= -\frac{\alpha_s C_A}{4\pi}\left[\frac{1}{\epsilon^2} - \frac{1}{\epsilon}\log\frac{-p_q^2 p_g^2}{\mu^2(p_q + p_g)^2} \right.$$
$$\left. + \frac{1}{2}\log^2\frac{-p_q^2 p_g^2}{\mu^2(p_q + p_g)^2} + \frac{\pi^2}{4} \right] \qquad (83)$$

$$= -\frac{\alpha_s C_A}{4\pi}\left[\frac{1}{\epsilon^2} - \frac{1}{\epsilon}\log\frac{-p_{\bar{q}}^2 p_g^2}{\mu^2(p_{\bar{q}}+p_g)^2}\right.$$
$$\left. + \frac{1}{2}\log^2\frac{-p_{\bar{q}}^2 p_g^2}{\mu^2(p_{\bar{q}}+p_g)^2} + \frac{\pi^2}{4}\right]. \quad (84)$$

Finally, we need the renormalization factor Z_A for the collinear gluon and Z_g for the coupling g_s which appears in the definition of $\mathcal{O}_3$;

$$Z_g^{-1} = \sqrt{Z_A} = 1 - \frac{\alpha_s}{4\pi}\left[\left(\frac{5}{6}C_A - \frac{n_f}{3}\right)\left(-\frac{1}{\epsilon} + \log\frac{-p_g^2}{\mu^2}\right)\right]. \quad (85)$$

However, since $Z_g\sqrt{Z_A} = 1$, these factors drop out of Z_3.

Adding up the diagrams, the $\frac{1}{\epsilon}\log p^2$ terms cancel, as they must. We find the renormalization factor for $\mathcal{O}_3$ at one loop is

$$Z_3 = 1 + \frac{\alpha_s}{4\pi}\left[C_F\left(\frac{2}{\varepsilon^2} + \frac{3}{\varepsilon} - \frac{2}{\varepsilon}\log\frac{-(p_q+p_{\bar{q}})^2}{\mu^2}\right)\right.$$
$$\left. + C_A\left(\frac{1}{\varepsilon^2} + \frac{1}{6\varepsilon} - \frac{1}{\varepsilon}\log\frac{-(p_q+p_g)^2(p_{\bar{q}}+p_g)^2}{\mu^2(p_q+p_{\bar{q}})^2}\right)\right], \quad (86)$$

and the anomalous dimension is

$$\gamma_3 = -\frac{\alpha_s}{\pi}\left[C_F\left(\log\frac{-\mu^2}{(p_q+p_{\bar{q}})^2} + \frac{3}{2}\right) + \frac{C_A}{2}\right.$$
$$\left. \times \left(\log\frac{-\mu^2(p_q+p_{\bar{q}})^2}{(p_q+p_g)^2(p_{\bar{q}}+p_g)^2} + \frac{1}{6}\right)\right]. \quad (87)$$

This is of the form (76), with

$$\Gamma_3 = C_F + \tfrac{1}{2}C_A, \quad (88)$$

$$B_3 = C_F\left(\frac{3}{2} - \log\frac{-(p_q+p_{\bar{q}})^2}{Q^2}\right)$$
$$+ \frac{C_A}{2}\left(\frac{1}{6} - \log\frac{-(p_q+p_g)^2(p_{\bar{q}}+p_g)^2}{Q^2(p_q+p_{\bar{q}})^2}\right). \quad (89)$$

Again, for leading-log resummation, only the cusp anomalous dimension Γ_3 is relevant.

3. Calculating the leading contribution to γ_n

As we have discussed earlier, only the cusp anomalous dimension is required for a LL resummation. The cusp anomalous dimension is the coefficient of the $1/\varepsilon^2$ counterterm and gets contributions from both soft and collinear diagrams. However, for every $1/\varepsilon^2$ divergent term in a particular diagram there is a term proportional to $(\log p^2)/\varepsilon$ which cannot be absorbed into a renormalization constant. As we found in the 2-jet matching at NLO, this term is canceled once the collinear and soft contribu-

tions are added. For the cancellation to occur, the total $1/\varepsilon^2$ terms from collinear diagrams have to be (-2) times the total $1/\varepsilon^2$ term of the soft diagrams. This implies that the LL contribution to the anomalous dimension γ_n can be obtained from collinear diagrams alone. Collinear fields in different directions do not interact with each other at leading order in SCET, thus the one-loop diagrams from collinear gluons only involve one collinear direction at a time. For example, the collinear diagrams required for the renormalization of $\mathcal{O}_2$ were a diagram involving only the collinear quark (Eqs. (61) and (67)), and the antiquark (Eqs. (62) and (67)). For the operator $\mathcal{O}_3$ an additional diagram involving the collinear gluon were required (Eq. (81) and (85)). Note the wave function graphs do not have $1/\varepsilon^2$ poles.

Combining these results, $1/\varepsilon^2$ poles in the counterterm of a general operator $\mathcal{O}_n$ with n_q quark fields and n_g gluon fields is

$$Z_n = 1 + \frac{\alpha_s}{4\pi}\left[\frac{n_q C_F + n_g C_A}{\varepsilon^2}\right] \quad (90)$$

which gives the anomalous dimension at LL order

$$\gamma_n = -\frac{\alpha_s}{2\pi}[n_q C_F + n_g C_A]\log\frac{\mu^2}{Q^2}. \quad (91)$$

Therefore, the cusp anomalous dimension for any operator in SCET is simply

$$\Gamma_n = \frac{n_q}{2}C_F + \frac{n_g}{2}C_A. \quad (92)$$

C. Threshold matching

Each collinear field from which the operators $\mathcal{O}_n$ are constructed can produce additional particles through interactions described by the Lagrangian of SCET. This implies that an operator $\mathcal{O}_n$ can contribute to final states with more than n partons. For example, we have used in the matching from QCD onto the operator $\mathcal{O}_3$ that the 3-parton matrix element of the operator $\mathcal{O}_2$ is nonvanishing, and it gave the dominant contribution for small values of p_T. However, in SCET only emissions which keep all external and internal partons near their mass shell are included, with the amount of virtuality allowed depending on the resolution scale of the effective theory. Since virtuality and transverse momentum are related, we use that only emissions with $p_T < \mu$ are allowed in SCET. This implies that if the scale μ gets lowered below the p_T of one of the final partons in the final state, the original matrix element no longer contributes to the final state, and a threshold matching onto an operator with an additional collinear field needs to be performed. The threshold matching condition for the operator $\mathcal{O}_2$ was already given in Eq. (20), and for a general operator $\mathcal{O}_n^{(j)}$

$$[C_n^{(j)}\langle\mathcal{O}_n^{(j)}\rangle]_{\mu=p_T+\varepsilon} = [C_{n+1}^{(j)}\langle\mathcal{O}_{n+1}^{(j)}\rangle]_{\mu=p_T-\varepsilon}. \quad (93)$$

We now work out explicitly the matching of $\mathcal{O}_2$ onto $\mathcal{O}_3^{(2)}$.

The threshold matching of $\mathcal{O}_2$ onto $\mathcal{O}_3^{(2)}$ occurs at a scale p_T. Actually, there are two relevant p_T scales for the branching: the transverse momentum of the gluon with respect to the quark, p_T^q, or to the antiquark, $p_T^{\bar{q}}$. However, since the SCET results are only valid in the limit $p_T \ll Q$, the two p_T's are interchangeable up to power corrections. So we use $p_T = \min(p_T^q, p_T^{\bar{q}})$. We might also consider p_T^g, the transverse momentum the quark (or antiquark) with respect to the gluon. But if p_T^g is the smallest transverse momentum, we are well outside of the validity of SCET, and this kinematical configuration is taken care of by the original matching to QCD. In fact, taking $p_T = \min(p_T^q, p_T^{\bar{q}}, p_T^g)$ is equivalent up to power corrections, and this quantity, to which spherocity reduces for 3-parton kinematics, has the added property of being infrared safe.

Above the scale $\mu = p_T$, the 3-parton matrix element of $\mathcal{O}_2$ is given by the sum of the two terms in Eq. (50)

$$\langle\mathcal{O}_2|q\bar{q}g\rangle = g_s\bar{\xi}_{n_q}\bigg[\slashed{A}\frac{\bar{\slashed{n}}_{\bar{q}}}{2}\frac{n_{\bar{q}}\cdot(p_q+p_g)}{(p_q+p_g)^2}\Gamma$$
$$-\Gamma\frac{n_q\cdot(p_{\bar{q}}+p_g)}{(p_{\bar{q}}+p_g)^2}\frac{\bar{\slashed{n}}_q}{2}\slashed{A}\bigg]\xi_{n_{\bar{q}}}. \quad (94)$$

Note that the $n\cdot(p+q)/(p+q)^2 = 1/\bar{n}\cdot(p+q)$ terms in Eq. (94) are due to the nonlocality of the intermediate quark propagator. However, the propagator scales as Q/p_T^2, and for $\mu < p_T$ the nonlocality of the propagator is less than the resolution of the theory. Thus, we can think of the matching of $\mathcal{O}_2$ onto $\mathcal{O}_3^{(2)}$ at $\mu = p_T$ as serving to keep the theory local by adding a label. This matrix element can be reproduced by the matrix element of an operator $\mathcal{O}_3^{(2)}$, defined as

$$\mathcal{O}_3^{(2)} = g_s\bar{\chi}_{n_q}\bigg[\slashed{A}_{n_g}\frac{\bar{\slashed{n}}_{\bar{q}}}{2}\frac{1}{\bar{n}_{\bar{q}}\cdot\mathcal{P}^\dagger}\Gamma - \Gamma\frac{1}{\bar{n}_q\cdot\mathcal{P}}\frac{\bar{\slashed{n}}_q}{2}\slashed{A}_{n_g}\bigg]\chi_{n_{\bar{q}}},$$
$$(95)$$

where χ_n is the same quark jet appearing in $\mathcal{O}_2$, and $\mathcal{A}_n^\mu$ is a gluon jet, that is a collinear gluon field wrapped in Wilson lines, as defined in (12). To satisfy the threshold matching condition we then find that the Wilson coefficient $C_3^{(2)}$ vanishes for $\mu > p_T$, and for $\mu = p_T$ it is equal to the Wilson coefficient of the operator $\mathcal{O}_2$

$$C_3^{(2)}(p_T) = C_2(p_T), \qquad C_3^2(\mu > p_T) = 0. \quad (96)$$

Using previous results, we can write

$$C_3^{(2)}(\mu) = C_2(Q)\Pi_2(Q, p_T)\Pi_3(p_T, \mu)\Theta(p_T - \mu). \quad (97)$$

Threshold matching is just another way of saying that $\mathcal{O}_2$ emits a gluon at $\mu = p_T$ and turns into $\mathcal{O}_3^{(2)}$. But it is important to understand the emission process as matching, so that it is improvable. For example, it would not be hard to do the threshold matching at next-to-leading order. This would involve calculating one-loop corrections to both the $\mathcal{O}_2$ emissions and to $\mathcal{O}_2^{(3)}$. The NLO matching would allow us to go beyond the strongly ordered limit $p_T^1 \gg p_T^2 \gg \cdots \gg p_T^n$, to which the parton shower is restricted, to correctly describe configurations with $p_T^1 \gg \cdots \gg p_T^j, p_T^{j+1} \gg \cdots \gg p_T^n$.

V. UNDERSTANDING THE SCET RESULTS

In the previous section, we worked out in detail some matching coefficients and evolution kernels in SCET. The important results were summarized in the beginning of that section. In this section, we will show how those results can be combined to obtain differential jet distributions and show that we agree with traditional perturbative calculations. We concentrate on the process $e^+e^- \to$ partons, whose kinematics are reviewed in Appendix B. If we work to order α_s we can have at most three partons in the final state (quark, antiquark, and gluon), and we can thus obtain the differential decay rate $d\sigma/(dsdt)$. We begin by showing the Sudakov factors used in parton showers are reproduced in SCET, and discuss the NLL resummation. We then show that the splitting functions are reproduced in the collinear limit. As a corollary, we derive within SCET the classical factorization that parton showers assume. We then discuss NLO results, and compare to QCD. Finally, we display results from SCET for the thrust distribution and the 2-jet fraction.

A. Sudakov factors from renormalization group evolution

First, we compare the RG evolution kernels obtained in the effective theory to the Sudakov factors which arise in traditional parton showers. We will show that to leading-log accuracy the evolution kernels coincide with traditional Sudakov factors. To start, suppose we just match from QCD to 2-jet operators. Then, according to (44), at $\mu = Q$, $C_2^{n,\bar{n}} = 1$ and all other Wilson coefficients vanish. For an emission at a scale p_T, we need to run C_2 down to $\mu = p_T$. Using the 2-jet anomalous dimension we find

$$C_2^{(n,\bar{n})}(\mu) = C_2(Q)\Pi_2(Q, \mu), \quad (98)$$

with the RG kernel given by

$$\Pi_2(Q, \mu) = \exp\bigg\{\frac{C_F}{\pi}\int_\mu^Q\frac{d\mu'}{\mu'}\alpha_s(\mu')\bigg[\log\frac{-\mu'^2}{Q^2} + \frac{3}{2}\bigg]\bigg\}. \quad (99)$$

This result can be compared with the expression for the Sudakov factor in traditional parton showers given in Eq. (7). The precise form of the Sudakov factor depends on the choice of evolution variables used, and on the

precise value of the argument of α_s that is used. Most Sudakov factors use for the scale of α_s an approximation to transverse momentum given by

$$\tau = z(1-z)t \approx p_T^2. \qquad (100)$$

As an example, we will consider the so-called NLL Sudakov [10,19,24], which also uses τ as the evolution variable. The limits of phase space are $\sqrt{\tau}/Q < z < 1 - \sqrt{\tau}/Q$. Thus the Sudakov factor becomes

$$\Delta_q^{\mathrm{NLL}}(\tau_2, \tau_1) = \exp\left\{-\frac{C_F}{2\pi}\int_{\tau_1}^{\tau_2}\frac{d\tau'}{\tau'}\alpha_s[\sqrt{\tau'}]\right.$$
$$\left.\times \int_{\sqrt{\tau'}/Q}^{1-(\sqrt{\tau'}/Q)}\mathrm{d}z\,\frac{1+z^2}{1-z}\right\}. \qquad (101)$$

The z integral can be evaluated analytically. Substituting $\mu = \sqrt{\tau'} \approx p_T$ gives

$$\Delta_q^{\mathrm{NLL}}(Q, \mu) = \exp\left\{\frac{C_F}{\pi}\int_\mu^Q \frac{d\mu'}{\mu'}\alpha_s(\mu')\left[\log\frac{\mu'^2}{Q^2}\right.\right.$$
$$\left.\left.+\frac{3}{2}+\mathcal{O}\left(\frac{\mu'}{Q}\right)\right]\right\}. \qquad (102)$$

Because the integral is dominated for small values of μ, we can drop the power law μ'/Q terms, as is done in the literature. Comparing (102) to (99) we see that the $\mathcal{O}(\alpha_s)$ evolution kernel reproduces this Sudakov factor exactly.

The $3/2$ term in (102) gives rise to subleading logarithms after integrating over μ, hence the name NLL Sudakov factor. However, there are additional subleading terms which are not included consistently. For example, changing the reference scale μ_R at which the renormalized α_s is defined gives rise to subleading terms which are also NLL. The optimal value of μ_R cannot be determined to the order we are working. Moreover, different Sudakov factors, based on different evolution variables, give a different constant term [10]. In other words, the Sudakov factor only gives the leading logarithms reliably, and the $3/2$ term may be dropped.

To illustrate this point, we show in Fig. 1 the 2-parton evolution kernel (Sudakov factor) Π_2 with various NLL effects included. The light band shows the effect of varying the $3/2$ term from 0 to 3. The darker band shows the effect of adding a NLL factor proportional to $\Gamma_2\alpha_s^2/(\pi^2)\times \log\mu'^2/Q^2$ to the integrand in Eq. (99), varying Γ_2 between 2 and -2. Note that the effect of the $3/2$ term and the NLL Γ_2 term are comparable at small μ. Since small μ is precisely where the Sudakov factors become important, it will be important to include all the NLL resummation in the Sudakov factors consistently. Later on, we will explore the NLL effects on the thrust distribution for 3-parton events (see Fig. 2).

For consistency we will therefore work only at leading-log accuracy, and drop the $3/2$ term. At LL all acceptable definitions of the Sudakov factors will give
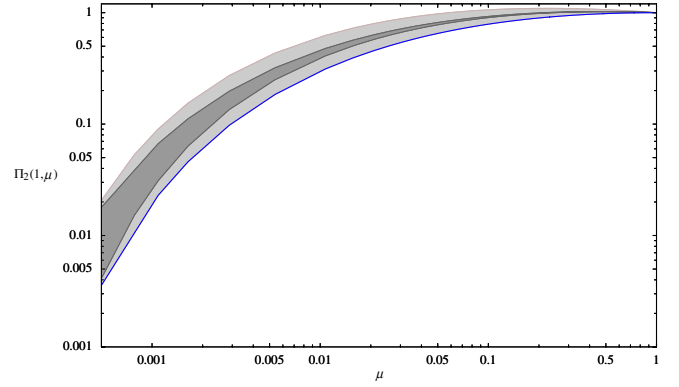

FIG. 1 (color online). Errors on the RG kernel (Sudakov factor) Π_2 from next-to-leading log uncertainties. The light band comes from one NLL effect, varying the $B_2^1\alpha_s$ term in the anomalous dimension, from $0 < B_2^1 < 3$. The dark band is from another NLL effect, the $\Gamma_2^2\alpha_s^2$ log term in γ_2, varying Γ_2^2 between -2 and 2. We normalize so that $\mu = 1$ corresponds to 1 TeV. The LO RG kernel is the lowermost curve in the figure.

$$\Delta_q^{\mathrm{LL}}(Q, \mu) = \exp\left\{\frac{C_F}{\pi}\int_\mu^Q \frac{d\mu'}{\mu'}\alpha_s(\mu')\log\frac{\mu'^2}{Q^2}\right\}, \qquad (103)$$

which is the LL SCET prediction as well. Analogously, the gluon Sudakov factor (the probability for a gluon not to branch) is given by [19]

$$\Delta_g^{\mathrm{LL}}(Q, \mu) = \exp\left\{\frac{C_A}{\pi}\int_\mu^Q \frac{d\mu'}{\mu'}\alpha_s(\mu')\log\frac{\mu'^2}{Q^2}\right\}. \qquad (104)$$

In SCET, the evolution kernel Π_n for an operator with n collinear fields is given by

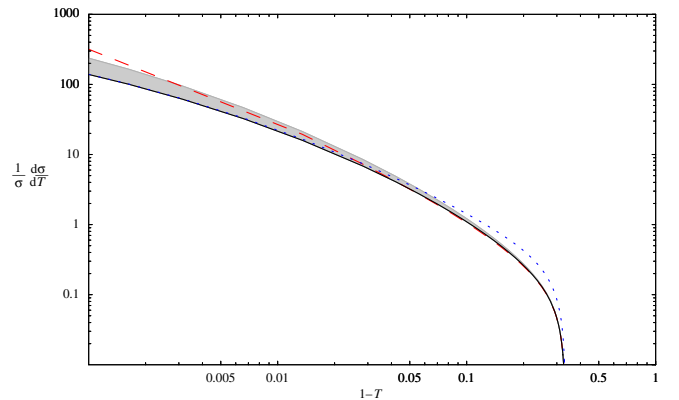$$\Pi_n(Q, \mu) = \exp\left\{-\int_\mu^Q \frac{d\mu'}{\mu'}\gamma_n(\mu')\right\}, \qquad (105)$$

FIG. 2 (color online). Thrust distribution from 3-parton states, at $E_{\mathrm{CM}} = 1$ TeV. QCD (dashed red line), parton-shower approximation (dotted blue line), and SCET (solid black line) are shown. The gray band is a representation of NLL uncertainties, by varying the B_2^1 and B_3^1 terms in γ_2 and γ_3, between 0 and their true values.

where $\gamma_n(\mu)$ is the anomalous dimension for the operator, given in Eq. (35). Comparing Eqs. (35) and (105) with Eqs. (103) and (104), we find that at LL accuracy the RG evolution kernel and the Sudakov factors are related according to

$$\Pi_n^2(Q, \mu) = \Delta_q^{n_q}(Q, \mu)\Delta_g^{n_g}(Q, \mu), \qquad (106)$$

where n_q (n_g) are the number of collinear quark (gluon) fields in the operator $\mathcal{O}_n$. Thus SCET reproduces all the classical Sudakov no-branching probabilities at leading log through the renormalization group flow of an effective theory.

B. Splitting functions from collinear emissions

In this section we will show how the couplings in SCET, when put into cross sections, reproduce the splitting functions of QCD.

For a 3-parton final state, once μ has run below p_T, the 2-jet operator can no longer contribute and the threshold matching turns $\mathcal{O}_2$ into $\mathcal{O}_3^{(2)}$. If we are not concerned with additional emissions, the differential cross section for emission will be

$$\frac{d\sigma}{dsdt} = \frac{\sigma_0}{64\pi^2} \sum_{\text{phys pols}} |C_3^{(2)}\langle\mathcal{O}_3^{(2)}|q\bar{q}g\rangle|^2, \qquad (107)$$

where

$$\sigma_0 = \frac{4\pi\alpha_e}{3Q^2}C_A\sum Q_j^2. \qquad (108)$$

We have already seen that $|C_3^{(2)}|^2$ encodes the Sudakov factor, so now let us look at the matrix elements. Using the explicit form of $\mathcal{O}_3^{(2)}$ given in Eq. (28), we can perform the sum explicitly. According to the conventions of Sec. IV, we find

$$|\langle\mathcal{O}_3^{(2)}\rangle|^2 = 8g_s^2C_F\left[\frac{s}{t}\frac{u^2+Q^2}{(s+t)^2} + \frac{t}{s}\frac{u^2+Q^2}{(s+t)^2}\right.$$
$$\left. + \frac{4Q^2u^2}{(t+u)(s+u)(s+t)^2}\right]. \qquad (109)$$

The first term comes from the square of the diagram with the quark emitting, the second from the square of the diagram with the antiquark emitting, and the third from interference.

Rewriting the amplitude in terms of t and z, and taking the limit where the gluon becomes collinear with the quark, so $p_T^{\bar{q}} \to 0$ and $t \to 0$, the amplitude approaches

$$\frac{d\sigma}{dsdt} = \frac{\sigma_0}{64\pi^2}|\langle\mathcal{O}_3^{(2)}\rangle|^2 = \sigma_0\frac{\alpha_s C_F}{2\pi}\frac{1}{t}\frac{1+z^2}{1-z} + \cdots, \qquad (110)$$

where the $\cdots$ are higher order in p_T/Q. So we reproduce the QCD splitting function (6), as required.

Note that the interference term (the third term in Eq. (109)) does not have an s or t pole, so it is finite as $p_T \to 0$ and represents a pure power correction. Since the interference is higher order in the SCET expansion, we may simply drop it. Recall that dropping interference terms is one of the approximations used in the parton shower, and so we see that it is justified by SCET. However, the interference term should be included following our conventions for evaluating matrix elements—if we dropped it, we would not reproduce QCD at the hard scale. Because we match at the matrix element level, it is important to keep the interference terms in. Note also that at leading order, we do not need to distinguish p_T^q from $p_T^{\bar{q}}$. We only know that p_T^q, $p_T^{\bar{q}} \ll Q$, which is where the SCET amplitude can be trusted.

We can also show that another element of parton showers, namely, that successive branchings factorize and may be treated classically, can be justified within SCET. Consider a general operator

$$\mathcal{O} = \bar{\chi}_n\Omega = \quad\longleftarrow\!\!\otimes \qquad (111)$$

where Ω contains any additional collinear fields and the Dirac structure of the operator. For example, for the operator $\mathcal{O}_2$ we would have $\Omega = \Gamma\chi_{\bar{n}}$. Now consider the emission of a collinear gluon off the collinear fermion χ_n. The amplitude for this process is given by

$$A = \bar{\chi}_n\mathcal{E}^\mu\Omega = \quad\overset{\text{\tiny oooo}}{\longleftarrow}\!\!\otimes \qquad (112)$$

where the emission $\mathcal{E}^\mu$ can be obtained from the Feynman rules of SCET. Explicitly,

$$\mathcal{E}^\mu = ig_sT^A\left[\frac{n_{\bar{q}}^\mu}{n_{\bar{q}}\cdot p_g} + \frac{1}{\bar{n}_{\bar{q}}\cdot(p_q+p_g)}\left(\bar{n}_{\bar{q}}^\mu + \frac{\not{p}_q^\perp\gamma_\perp^\mu}{n_{\bar{q}}\cdot p_q}\right)\right]. \qquad (113)$$

The first term comes from the Wilson line emission[3] and the second from the vertex in the SCET Lagrangian. An important property of $\mathcal{E}^\mu$ is that its square has trivial Dirac structure. In fact,

$$\mathcal{E}_\mu^\dagger\mathcal{E}^\mu = 2g_s^2C_F\frac{2u(Q^2-s)+t^2}{stu} \times \text{id}_{4\times4}$$
$$\to 8g_s^2C_F\frac{1}{z}\frac{1}{t}\frac{1+z^2}{1-z} \times \text{id}_{4\times4}. \qquad (114)$$

The arrow represents the collinear $t \to 0$ limit, where we see that QCD splitting function $P(t, z)$ appears (cf. Eq. (5)), with an extra factor of $1/z$. Now, consider squaring the amplitude A and summing over spins. The spin sum gives a

---

[3]We include the Wilson line emission here, in contrast to our previous conventions, to insure gauge invariance. The same results hold if we ignore the Wilson line but only sum over physical polarizations.

factor of $\not{p}_q$, which in the collinear limit is $\not{p}_q = z\not{n}$, which commutes with $\mathcal{E}^\mu$. So,

$$|A|^2 = \text{Tr}\{\not{q}\mathcal{E}^\mu \Omega \Omega^\dagger \mathcal{E}^\dagger_\mu\} = z\,\text{Tr}\{\mathcal{E}^\dagger_\mu \mathcal{E}^\mu \not{n}\Omega \Omega^\dagger\}.$$

Since $\mathcal{E}^\dagger_\mu \mathcal{E}^\mu$ is proportional to the identity matrix in spinor space, we can pull it out of the trace to obtain the final result

$$|A|^2 = 64\pi^2 P(t, z)\,\text{Tr}\{\mathcal{O}\mathcal{O}^\dagger\}. \tag{115}$$

This shows that, in the collinear limit, the amplitude for a quark to branch into a quark and a gluon is independent of the other fields in the process, and that the probability for branching is given by a splitting function.

Having considered a single emission of a gluon, we can go one step further and allow for multiple emissions. If we call $p_T^{(j)}$ the transverse momentum of the emitted gluon with respect to its mother particle, the multiple emissions can be treated as a succession of threshold matchings if

$$p_T^{(1)} \gg p_T^{(2)} \gg p_T^{(3)} \gg \dots . \tag{116}$$

This ordering of transverse momenta is called the strongly ordered limit. In that case, the first emission is encoded in the threshold matching from $\mathcal{O}_2$ onto $\mathcal{O}_3^{(2)}$, the next emission in the matching from $\mathcal{O}_3^{(2)}$ onto $\mathcal{O}_4^{(2)}$, and so on. Since in the above calculation we have assumed a general operator $\bar\chi_n\Omega$, the results can be applied recursively to the square of the final operator $\mathcal{O}_n^{(2)}$ that is obtained after all the threshold matchings are performed. Thus, the square of the final operator in the strongly ordered limit can be written as the square of the original operator $\mathcal{O}_2$, multiplied by products of splitting functions. This is precisely the result that a parton-shower algorithm would give for the same process, proven within SCET.

C. Comparison with full QCD perturbative results

In this section, we will show how the SCET results produce cross sections which agree with QCD at next-to-leading order. We begin by calculating the most inclusive of quantities, the total cross section for $e^+e^- \to$ partons, at NLO. This will incorporate the NLO matching of C_2 and the 2-jet anomalous dimension. It shows that all the $\mathcal{O}(\alpha_s)$ information from QCD is in fact contained in the effective theory. Then we consider the differential decay rate $d\sigma(e^+e^- \to q\bar{q}g)$, also at NLO [39–47]. First, we reproduce the $1/\varepsilon$ and $1/\varepsilon^2$ divergences in this rate from the counterterms in SCET. Then we show that at $\mathcal{O}(\alpha_s)$ all of the large logarithms, which appear in the limit $p_T \ll Q$, are resummed.

We begin with the total cross section at NLO. This total cross section receives contributions from both 2- and 3-parton final states, and the 2-parton states have to be calculated to one-loop accuracy, while for the 3-parton final states only tree level is required [25,26]. In the effective theory this means that to work consistently at order α_s

we need the one-loop matching for C_2 and the tree-level matching for C_3. We also need the one-loop matrix element for $\mathcal{O}_2$ and tree-level matrix element for $\mathcal{O}_3$. Both the 2- and 3-parton cross sections σ_2 and σ_3 are infrared divergent, but these infrared divergences cancel in the sum of the two terms.

We begin by calculating the 3-parton cross section σ_3. In SCET it is obtained by squaring the amplitude $C_2\langle\mathcal{O}_2|q\bar{q}g\rangle + C_3\langle\mathcal{O}_3|q\bar{q}g\rangle$. Because of the matching condition (46), this amplitude is exactly equal to the QCD amplitude. Thus, regulating the IR divergence in dimensional regularization, the 3-jet rate is

$$\sigma_3^{\text{SCET}} = \int d\sigma_3^\varepsilon$$

$$= \sigma_2^\varepsilon \frac{\alpha_s C_F}{2\pi}\left(\frac{2}{\varepsilon^2} + \frac{3}{\varepsilon} + \frac{2}{\varepsilon}\log\frac{\mu^2}{Q^2} + \log^2\frac{\mu^2}{Q^2}\right.$$

$$\left. + 3\log\frac{\mu^2}{Q^2} + \frac{19}{2} - \frac{7\pi^2}{6}\right), \tag{117}$$

where we have written the result in terms of the $\mathcal{O}(\alpha_s^0)$ 2-parton cross section with dimensionally regulated phase space

$$\sigma_2^\varepsilon = \sigma_0\left(\frac{4\pi}{Q^2}\right)^\varepsilon \frac{3(1 - \varepsilon)\Gamma(2 - \varepsilon)}{(3 - 2\varepsilon)\Gamma(2 - 2\varepsilon)}. \tag{118}$$

For the 2-parton cross section we require both the Wilson coefficient C_2 and the matrix element $\langle\mathcal{O}_2|q\bar{q}\rangle$ at one loop. Since the 3-parton rate above was calculated for an arbitrary renormalization scale μ we need the Wilson coefficient at that scale. Combining Eqs. (66) with $\Pi_2(Q, \mu)$ we find

$$C_2(\mu) = C_2(Q)\Pi_2(Q, \mu)$$

$$= 1 - \frac{\alpha_s C_F}{4\pi}\left[8 - \frac{\pi^2}{6} + \log^2\frac{-\mu^2}{Q^2} + 3\log\frac{-\mu^2}{Q^2}\right]. \tag{119}$$

We also need the matrix element of the operator $\mathcal{O}_2$ at one loop. In pure dimensional regularization, the one-loop contribution to the bare matrix element vanishes, since in the effective theory all large scales have been removed from the theory and all infrared scales are set to zero. Thus, the only contribution to the matrix element comes from the renormalization factor, given in Eq. (68)

$$Z_2 = 1 + \frac{\alpha_s C_F}{4\pi}\left[\frac{2}{\varepsilon^2} + \frac{3}{\varepsilon} + \frac{2}{\varepsilon}\log\frac{-\mu^2}{Q^2}\right]. \tag{120}$$

Combining these results, the 2-parton cross section is

$$\sigma_2^{\text{SCET}} = \sigma_2^\varepsilon |C_2 \langle \mathcal{O}_2 | qq \rangle|^2 = \sigma_2^\varepsilon \left| C_2 \frac{1}{Z_2} \langle \mathcal{O}_2 | qq \rangle^{\text{bare}} \right|^2$$

$$= \sigma_2^\varepsilon \left[1 - \frac{\alpha_s C_F}{2\pi} \left(\frac{2}{\varepsilon^2} + \frac{3}{\varepsilon} - \frac{7\pi^2}{6} + 8 + 2 \frac{\log \frac{\mu^2}{Q^2}}{\varepsilon} \right. \right.$$
$$\left. \left. + \log^2 \frac{\mu^2}{Q^2} + 3 \log \frac{\mu^2}{Q^2} \right) \right],$$

where we have used $\langle \mathcal{O}_n \rangle = Z_n^{-1} \langle \mathcal{O}_n \rangle^{\text{bare}}$.

The sum of the 2-parton and 3-parton contributions is finite, and we find for the total cross section to order α_s

$$\sigma_{\text{tot}} = \sigma_2^{\text{SCET}} + \sigma_3^{\text{SCET}} = \sigma_0 \left(1 + \frac{3\alpha_s}{4\pi} C_F \right), \quad (121)$$

which is the standard QCD result, reproduced in SCET.

There is an easy way to see why σ_2 came out the same as in QCD. In QCD, the virtual contribution to the 2-parton cross section is UV finite. Thus, in dim reg, all the ε dependence comes from IR divergences. But the IR divergences in QCD are the same as in SCET. In SCET, no divergences appear at all when using dim reg, because there are no scales in the problem. Equivalently, in SCET the UV and IR divergences precisely cancel. So the IR divergences are equal to the UV divergences which can be extracted from the counterterm. Thus, the counterterm in SCET has all the information about the full dimensionally regulated QCD answer, up to finite terms. And these finite terms are precisely what is calculated in the matching. Just as SCET reproduces the virtual contribution to σ_2 from QCD, it is also capable of reproducing the NLO contribution to $d\sigma_3$. In QCD, this computation involves all one-loop contributions to $e^+e^- \to qqg$. Again, there are IR divergences, which are canceled when σ_4, the integral of tree-level 4-parton emission, and the 2-loop contribution to σ_2 are added. In this paper, we have not included all of the relevant computations to reproduce σ_3 at NLO completely, however we have enough information to reproduce all of the infrared divergences, as well as the dominant large logarithms in the finite part.

The next-to-leading order QCD result for the dimensionally regularized 3-parton differential cross section can be found in [39,40]. Consider first the divergent terms. They are all proportional to the tree-level cross section and are contained in

$$d \sigma_3^{\text{QCD}_1} = d\sigma_3^\varepsilon \frac{\alpha_s}{2\pi} \left(\frac{4\pi\mu^2}{Q^2} \right)^\varepsilon \left\{ -\frac{C_A + 2C_F}{\varepsilon^2} - \frac{1}{\varepsilon} \left[3C_F \right. \right.$$
$$\left. \left. + \frac{\beta_0}{2} - 2C_F \log \frac{u}{Q^2} - C_A \log \frac{st}{uQ^2} \right] \right\} + \cdots$$
$$(122)$$

The SCET prediction for the 3-parton cross section comes from

$$d\sigma^{\text{SCET}} = \text{PS}_3^\varepsilon \times |C_2 \Pi_2(Q, p_T) \Pi_3(p_T, \mu) \langle \mathcal{O}_3^{(2)} | q\bar{q}g \rangle$$
$$+ C_3 \Pi_3(Q, \mu) \langle \mathcal{O}_3 | q\bar{q}g \rangle|^2, \quad (123)$$

where PS_3^ε refers to the dimensionally regulated 3-parton phases space. The $1/\varepsilon^2$ and $1/\varepsilon$ poles in QCD come from soft and/or collinear IR divergences in the matrix elements. In pure dim reg, the bare matrix elements vanish in SCET, since the UV and IR divergences cancel. Therefore all the poles show up as UV divergences contained in the renormalization constants. Expanding,

$$\langle \mathcal{O}_3 | q\bar{q}g \rangle \propto \frac{1}{Z_3} \langle g_s q\bar{q}g | q\bar{q}g \rangle^{\text{bare}} = \frac{Z_g}{Z_3} g_s \langle q\bar{q}g | q\bar{q}g \rangle^{\text{bare}}.$$
$$(124)$$

Thus, at NLO, the poles are extracted from Eq. (123) by using Z_g and Z_3 at $\mathcal{O}(\alpha_s)$ and setting $\Pi_2 = \Pi_3 = C_2 = C_3 = 1$. At order $\mathcal{O}(\alpha_s)$, the counterterms pulled from Eqs. (85) and (86), give

$$\frac{Z_g}{Z_3} = 1 - \frac{\alpha_s}{4\pi} \left[\frac{2C_F + C_A}{\varepsilon^2} + \frac{1}{\varepsilon} \left(3C_F + \frac{\beta_0}{2} - 2C_F \log \frac{-u}{Q^2} \right. \right.$$
$$\left. \left. - C_A \log \frac{-st}{uQ^2} + (2C_F + C_A) \log \frac{-\mu^2}{Q^2} \right) \right]. \quad (125)$$

As expected, $|Z_3^{-1}|^2$ reproduces all of the divergences of the QCD expression. Note that the matrix elements for $\mathcal{O}_3$ and $\mathcal{O}_3^{(2)}$ reproduce QCD, by the matching conditions, so we get the same $d\sigma_3^\varepsilon$ factor in both cases. The other part of the QCD expression we should be able to reproduce are the dominant large logarithms. For the logs to be large, we need $p_T \ll Q$. In this limit, SCET is a good approximation to QCD, and $\langle \mathcal{O}_3 | q\bar{q}g \rangle \approx 0$. Then the large logs should be resummed in the Wilson coefficients, through the Π_2 factor. To order α_s,

$$\Pi_2(Q, \mu) = 1 - \frac{\alpha_s C_F}{4\pi} \left[\log^2 \frac{\mu^2}{Q^2} + (3 + 2i\pi) \log \frac{\mu^2}{Q^2} \right]. \quad (126)$$

For $p_T \ll Q$, $\mu = p_T \sim \frac{\sqrt{stu}}{Q^2}$ (see Appendix B) and the kinematical structure of the SCET cross section is that of a splitting function. Thus,

$$\frac{d\sigma_3^{\text{SCET}}}{dsdt} = \frac{\sigma_0}{64\pi^2} |C_2(Q) \Pi_2(Q, p_T) \langle \mathcal{O}_2 | q\bar{q}g \rangle|^2 + \cdots$$
$$= \sigma_0 P(t, z) \left[1 - \frac{\alpha_s C_F}{2\pi} \left(\log^2 \frac{stu}{Q^6} + 3 \log \frac{stu}{Q^6} \right) \right]$$
$$+ \cdots \quad (127)$$

To compare to the QCD result, we need to extract all the relevant terms from the NLO QCD expression [39]. Since we can only reproduce the logarithmically enhanced terms at this order, we will work in the kinematic limit $t \ll s, u$ and expand the full QCD result in powers of t. First, there is a contribution from the pieces with the kinematics of the

tree-level cross section. This includes the finite piece from Eq. (122), evaluated at $\mu = stu$, and an additional finite piece from [39]. All the terms from these expressions with $\log t$ are

$$\frac{d\sigma_3^{\text{QCD}_1}}{dsdt} = \sigma_0 \frac{\alpha_s C_F}{2\pi} \frac{s^2 + t^2 + 2uQ^2}{st} \frac{\alpha_s}{2\pi}$$
$$\times \left[C_F \left(\log^2 \frac{stu}{Q^6} - 3 \log \frac{stu}{Q^6} \right) \right.$$
$$\left. + \log \frac{stu}{Q^6} \left(-\frac{\beta_0}{2} + (2C_F - C_A) \log \frac{u}{Q^2} \right) \right]. \quad (128)$$

Next, there is a part of the QCD expression which is not proportional to $d\sigma_3$, but has a splitting function as its collinear limit. Its large logs are

$$\frac{d\sigma_3^{\text{QCD}_2}}{dsdt} = \sigma_0 \frac{\alpha_s C_F}{2\pi} \frac{u^2 + (s + u)^2}{st}$$
$$\times \left[-(2C_F - C_A) \log \frac{t}{Q^2} \log \frac{u}{Q^2} \right]. \quad (129)$$

Finally, there is a contribution from the running of α_s. The SCET expression is evaluated with $\alpha_s(\mu)$ while the QCD expression with $\alpha_s(Q)$. Changing the scale for the QCD expression gives an extra factor:

$$\frac{d\sigma_3^{\text{QCD}_3}}{dsdt} = \sigma_0 \frac{\alpha_s(\mu) C_F}{2\pi} \frac{s^2 + t^2 + 2uQ^2}{st}$$
$$\times \left[\frac{\alpha_s}{2\pi} \frac{\beta_0}{2} \log \frac{stu}{Q^6} \right]. \quad (130)$$

Taking the $t \to 0$ limit of these three expressions and adding them we find

$$\frac{d\sigma_3^{\text{QCD}}}{dsdt} = \sigma_0 \frac{\alpha_s C_F}{2\pi} \frac{1}{t} \frac{1 + (1 - s)^2}{s}$$
$$\times \left[1 - \frac{\alpha_s C_F}{2\pi} \left(\log^2 \frac{stu}{Q^6} + 3 \log \frac{stu}{Q^6} \right) \right], \quad (131)$$

which matches the SCET expression in Eq. (127). Thus SCET resums all the large logarithms.

There are terms in the full QCD expression with logs of u/Q^2. In configurations with $u \ll Q$ either the quark and antiquark are back to back, or one of them soft. These configurations do not come from soft or collinear emission from $\mathcal{O}_2$, and thus the large logs of u/Q^2 are not resummed by Π_2. However, large logs of u are resummed in Π_3; and once SCET incorporates all the one-loop matching, all of these terms, as well as all of the finite terms in the QCD expression, should be accounted for.

D. Interpolating between QCD and parton showers

A useful way to explore the SCET prediction is by looking at infrared-safe observables. We will compare QCD, parton showers, and SCET. Since we only worked out results for e^+e^- to 2 or 3 partons, we can only compute

observables that depend on the 3-parton differential distribution. Once SCET is incorporated into a full event generator, more complicated events can be produced. But the results of this section are sufficient to show, at least conceptually, how SCET interpolates between QCD and the parton shower. So we take our observables to be functions of the 3-parton kinematics: $f(s, t)$. For example, thrust is

$$T(s, t) = 1 - \frac{1}{Q^2} \min\{s, t, 1 - s - t\}. \quad (132)$$

Now, let us consider the 3 cases in turn.

First, take tree-level QCD prediction. Thrust is computed as

$$\frac{1}{\sigma_0} \frac{d\sigma^{\text{QCD}}}{dT} = \frac{\alpha_s C_F}{2\pi} \int dsdt \frac{s^2 + t^2 + 2uQ^2}{st} \delta(T - T(s, t)). \quad (133)$$

The prediction for QCD at NLO would be the same, but normalized to the NLO total cross section $\sigma_0(1 + \frac{\alpha_s}{\pi})$ instead of just σ_0.

The parton-shower (PS) prediction, which resums the leading logs, is given by

$$\frac{1}{\sigma_0} \frac{d\sigma^{\text{PS}}}{dT} = \int dsdt [\Delta(Q, p_T^q)^2 P(t, z)$$
$$+ \Delta(Q, p_T^{\bar{q}})^2 P(s, z')] \delta(T - T(s, t)), \quad (134)$$

where $P(t, z)$ is the splitting function from the quark emission, and $P(s, z')$ is the splitting function from the antiquark emission (here, $z = \frac{Q^2 - s}{Q^2 + t}$ and $z' = \frac{Q^2 - t}{Q^2 + s}$).

Finally, the SCET prediction is

$$\frac{1}{\sigma_0} \frac{d\sigma^{\text{SCET}}}{dT} = \frac{1}{64\pi^2} \int dsdt |C_2 \Pi_2(Q, p_T) \langle \mathcal{O}_3^{(2)} | q\bar{q}g \rangle$$
$$+ C_3 \Pi_3(Q, p_T) \langle \mathcal{O}_3 | q\bar{q}g \rangle|^2 \delta(T - T(s, t)). \quad (135)$$

To evaluate this we use the evolution kernels Π_2 and Π_3 from Eq. (38) with Eqs. (33) and (34) and the matrix elements. The matrix element for $\mathcal{O}_3^{(2)}$ is given in Eq. (109):

$$|\langle \mathcal{O}_3^{(2)} \rangle|^2 = 8g_s^2 C_F \left[\frac{(s^2 + t^2)(u^2 + Q^2)}{st(s + t)^2} \right.$$
$$\left. + \frac{4Q^2 u^2}{(t + u)(s + u)(s + t)^2} \right]. \quad (136)$$

The others (evaluated with the conventions of Sec. IV) are

$$|\langle \mathcal{O}_3 | q\bar{q}g \rangle|^2 = 16g_s^2 C_F \frac{u^2(s^2 + t^2)}{(t + u)(s + u)(s + t)^2}, \quad (137)$$

$$\langle q\bar{q}g | \mathcal{O}_3^{(2)} \rangle \langle \mathcal{O}_3^\dagger | q\bar{q}g \rangle + \text{H.c.}$$
$$= -16g_s^2 C_F \frac{u^2(s^2 + t^2) - 2stu}{(t + u)(s + u)(s + t)^2}. \quad (138)$$

Note that the only term that has infrared s or t poles is Eq. (136). The others are finite, and not genuine predictions of SCET. They depend only on our conventions. If it were possible to choose consistent conventions so that $\langle \mathcal{O}_3 | q\bar{q}g \rangle = 0$, then only $\langle \mathcal{O}_2^{(3)} | q\bar{q}g \rangle$ would contribute to the distribution, and because of the matching, it would be the same as QCD. In this case, our distribution would be a Sudakov factor, Π_2^2 multiplying the QCD cross section, which is just the prescription of CKKW [19]. So our prediction, at this order, is equivalent to theirs, up to power corrections. Nevertheless, we cannot simply choose $\langle \mathcal{O}_3 | q\bar{q}g \rangle = 0$, because we need a consistent set of conventions which allow us to go to higher orders.

The thrust distribution for these three approaches is shown in Fig. 2. We also include in this figure the NLL uncertainties as a gray band. This band corresponds to varying the B_2 and B_3 terms in the anomalous dimensions between 0 and their true values. Although the true value is known, this variation represents the NLL uncertainty from the Γ_2^2 and Γ_3^2 terms, which multiply $\alpha_s^2 \log \mu$ in γ_2 and γ_3, and which is not known. Confer Fig. 1 as well.

There are two important features of Fig. 2 worth observing. First, note how SCET interpolates between QCD and PS. Small thrust, which corresponds to large p_T, is populated by events with hard jets. In this region, we expect QCD to be a good approximation, as there are no large logarithms, and PS to be a bad approximation, as we are away from the collinear limit where splitting functions are derived. Note that SCET approaches QCD in this region. In contrast, large thrust is determined by events with soft or collinear partons. Here, tree-level QCD is inaccurate, because of large logarithms, while the PS is closer to reality. SCET matches the parton shower here. So SCET smoothly interpolates between QCD and PS.

The second feature worth noting is the effect of the NLL resummation. Notice how the gray band is large for $T \sim 1$, which is where the PS is supposed to be accurate. Thus it seems the PS is valid neither at small T, where hard emissions dominate, nor at large T, where NLL resummation is important. In contrast SCET is valid at small T, but also, once all NLL effects are consistently incorporated, it has the potential to be accurate in all regimes. This shows that resumming next-to-leading logs may be crucial to get accurate distributions.

Next we compute the 2-jet rate. To do this we need a jet definition [48]. We will use the k_T (Durham) algorithm [24]. It defines for any two partons a and b

$$y^{ab} \equiv \frac{2}{Q^2} \min\{E_a^2, E_b^2\}(1 - \cos\theta_{ab}) > y_{\text{cut}}. \quad (139)$$

We then use

$$y \equiv \min\{y^{qg}, y^{\bar{q}g}, y^{q\bar{q}}\}. \quad (140)$$

For a 3-parton configuration, if $y > y_{\text{cut}}$, there are more than 2 jets, otherwise there are only 2. Thus we compute
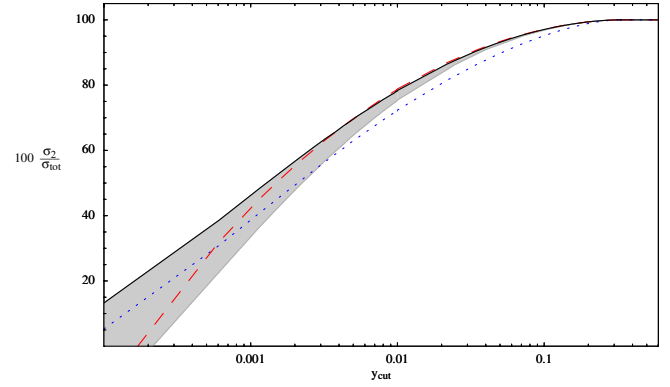

FIG. 3 (color online).   Percentage of events which have 2 jets, as a function of cutoff, using the k_T algorithm. Shown is QCD (dashed red line), the parton-shower approximation (dotted blue line), and SCET (solid black line). The gray band is the NLL uncertainty, as in Fig. 2.

the 2-jet rate by integrating the distributions for QCD, SCET, and parton showers, over the appropriate range. We avoid the infrared singularities by integrating over events with $k_T > y_{\text{cut}}$. For example,

$$\sigma_2^{\text{QCD}}(y_{\text{cut}}) = \sigma_{\text{tot}} - \frac{\alpha_s C_F}{2\pi}$$
$$\times \int ds dt \frac{s^2 + t^2 + 2uQ^2}{st} \Theta(y - y_{\text{cut}}). \quad (141)$$

The results for this observable are shown in Fig. 3. The effect of the Sudakov suppression can be seen on the left side, at small y_{cut}. Here, the tree-level QCD prediction drops below zero, showing that its estimate of σ_2 is no longer trustworthy. Both the PS and the SCET curves are still positive at low energy, implying that they give a better estimate of the 2-jet cross section. For large y_{cut}, the 2-jet rate should be accurately given by QCD. The PS gets the rate wrong, because it is integrating over hard emission where it is not valid. The finite difference between the PS and SCET curves comes from the integral over large p_T, where the PS cannot be trusted.

VI. TOWARDS SCET EVENT GENERATION

We have shown in the previous section that SCET reproduces parton showers, Sudakov suppression, and NLO QCD results, and that it smoothly interpolates between the hard and soft regimes where QCD and parton showers are valid. In this section we will illustrate how the SCET formalism is naturally suited to implementation in an event generator. It has the capacity to produce particle distributions with several high p_T jets, while summing the leading logarithms. And it is at least as powerful as parton showers for recursively adding additional soft or collinear partons. What we are after is the differential cross section $d\sigma$ for events with an arbitrary number of final states. In an event generator, this amounts to computing the weight, or

probability, of an event, given the kinematics of the particles in the event. We will review schematically the analytical expressions required and give a simple algorithm to obtain events distributed according to these distributions.

A. Analytical distributions

Suppose we want the weight for an event with r particles from a production process at center-of-mass energy Q. To calculate this, the SCET approach requires a sequence of matching and running steps. First QCD is matched onto SCET at the scale $\mu = Q$ by requiring that matrix elements with a given number of particles are correctly reproduced by the effective theory. In practice, how many particles we include depends on the number of matrix elements that it is feasible to compute in full QCD (and in SCET). This will in general be much less than r. Let m be the maximum number of partons which are matched. So the matching turns on operators $\mathcal{O}_2$ through $\mathcal{O}_m$ at $\mu = Q$. After the matching, each of the operators is evolved to lower scales using the renormalization group equations. To do this, we need the threshold matching scales, $p_T^{(i)}$, which can be derived from the event's momenta, for example, with the k_T algorithm [24]. So we have $p_T^{(1)} > p_T^{(2)} > \cdots > p_T^{(r)}$. At $\mu \sim p_T^{(1)}$ a threshold matching is performed where the operator $\mathcal{O}_2$ is matched onto an operator $\mathcal{O}_3^{(2)}$. The set of operators is then evolved to the scale $\mu \sim p_T^{(2)}$, at which scale the operators $\mathcal{O}_3$ and $\mathcal{O}_3^{(2)}$ are matched onto $\mathcal{O}_4^{(3)}$ and $\mathcal{O}_4^{(2)}$. This continues until the scale μ reaches the scale $\mu = \Lambda_{\text{IR}}$. The differential cross section is then (up to phase space factors)

$$
\begin{aligned}
\mathrm{d}\,\sigma_r &= \left| \sum_{j=2}^m \mathrm{C}_r^{(j)}(\mu)\mathcal{O}_r^{(j)} \right|^2 \\
&= |[C_2(Q)\Pi_2\Pi_3\cdots\Pi_r]\mathcal{O}_r^{(2)} \\
&\quad + [C_3(Q)\Pi_3\cdots\Pi_r]\mathcal{O}_r^{(3)} + \cdots \\
&\quad + [C_m(Q)\Pi_m\cdots\Pi_r]\mathcal{O}_r^{(m)}|^2.
\end{aligned}
\tag{142}
$$

Note that since only operators $\mathcal{O}_j$ with $j \le m$ were included in the matching onto SCET, this expression will only reproduce the full QCD results exactly with up to m partons in the final state. All additional partons are described by radiation in SCET and thus rely on an expansion in p_T. As we have shown, after squaring the matrix elements, the SCET radiation is equivalent to the splitting functions used in parton showers. So,

$$
\mathrm{d}\,\sigma_{r>m} = \mathrm{d}\sigma_m \times \text{parton shower.}
\tag{143}
$$

This distribution will be valid if the p_T satisfy

$$
p_T^{(1)}, \cdots, p_T^{(m)} \gg p_T^{(m+1)} \gg \cdots \gg p_T^{(r)}.
\tag{144}
$$

So if we want the distribution for r hard jets, we should aim for $m \ge r$.

B. A sample algorithm

Now let us consider how to incorporate these results into an event generator. This means we need an algorithm for sampling the phase space and unweighting events. We do not intend to present a complete or ideal solution, but rather sketch one possibility. Suppose that we have QCD and SCET matrix elements for up to m partons, then an algorithm might look like

(1) Start with a hadronic event at center-of-mass energy Q, according to as accurate calculations of total cross sections as are available.
(2) Pick a configuration of m partons with probability proportional to $\mathrm{d}\sigma_m$ in Eq. (142).
(3) If the minimum p_T of the configuration, $p_T^{(m-2)}$ is more than IR cutoff Λ_{IR}, then we have an event with m or more partons.
    (i) Start a parton shower at $\mu = p_T^{(m-2)}$, using the SCET RG kernels as Sudakov factors.
(4) Otherwise, we have an event with less than m partons.
    (a) Pick momenta for $m - 1$ partons with probability proportional to $\mathrm{d}\sigma_{m-1}$ in Eq. (142).
    (b) If the minimum p_T of this configuration, $p_T^{(m-3)}$ is more than the IR cutoff Λ_{IR}, then we have an event with $m - 1$ partons.
        (i) Do not shower. Go straight to hadronization with this kinematics. Or, equivalently, shower starting at $\mu = \Lambda_{\text{IR}}$.
    (c) Otherwise, we have an event with less than $m - 1$ partons. Return to step (a) with $m \to m - 1$.

There are several points worth elaborating on here. First, note that the differential distributions in SCET do not diverge as two partons become collinear or one becomes soft. This is because we are not using the QCD amplitude and correcting with Sudakov factors later on, but using the SCET amplitude which has the Sudakov suppression built in. Since the Sudakov factor vanishes exponentially in either of these limits, it overcomes the linear power divergence present in the full QCD amplitude.

Second, although we need to use some type of jet definition to sort the p_T in the kinematics, there will be only a very weak dependence on this definition in the final results. The strongest dependence on the jet definition should cancel from matching to the hadronization routine. The detailed sorting of p_T only has an effect on momenta which are strongly ordered, in which case all infrared-safe jet definitions should agree. There may be a subleading effect, which amounts to power corrections, and is beyond the order we are working. Also note that because the amplitude is finite even for small p_T, we do not need to employ an intermediate jet cutoff scale in the theory, between Q and Λ_{IR}. We emphasize that this algorithm produces fully exclusive events, independent of jet definition. For observables with jets, the events can be combined

using whatever algorithm is desired, and if the same algorithm is used on the data there should be good agreement.

Third, if we are working to a consistent order in α_s, the distribution in step VI B should really be done at NLO for $m - 1$ partons, and NNLO for $m - 2$ partons, etc. As we have shown, all the NLO information from QCD can be reproduced in SCET, but one still needs to integrate over the regulated phase space for m partons in the singular region to cancel the NLO divergences for the $m - 1$ parton event. The details of the implementation of the NLO effects will be left for future work. Finally, the reason we do not just skip step VI B is as follows. The distribution of m partons, from steps 1 through 3, is as accurate as possible with the information given. But because of the Sudakov suppression, the amplitude to produce fewer than m jets is probably very small. In fact, in steps 1 to 3, we make a Monte Carlo estimate of the m-or-more parton cross section. The distribution at small p_T is also sensitive to subleading logarithms, and so we probably cannot trust it. Therefore, step 4 recalculates the distribution from the hard scale, which should be a better estimate of the $m - 1$ parton event shape.

VII. CONCLUSION

We have shown how to construct an event generator based on effective field theory. The correct effective theory reproducing all collinear and soft divergences of QCD is SCET, and we have shown that SCET at leading order is equivalent to a conventional parton shower. The advantage over the parton shower is that an effective theory is systematically improvable order by order. In particular, we have shown that by matching SCET onto QCD matrix elements with up to three partons allows to obtain cross sections which smoothly merge the parton-shower approximation with more accurate matrix elements for events with large transverse momentum. Since we have a consistent effective field theory framework for the shower, we know precisely to what order we are working. We can therefore estimate errors, and then incorporate higher-order corrections if necessary when comparing to data. There are five places where higher-order corrections can be incorporated

   (1) Matching to QCD for higher multiplicity matrix elements.
   (2) Matching to QCD at higher loop order.
   (3) Higher loop running.
   (4) Matching within SCET across the emission threshold, at higher order.
   (5) Power corrections from the SCET expansion.

The first three we have already discussed at length in this paper. Of these the higher loop running may be the most important to work out and implement. We showed in Figs. 1 and 2 an estimate of NLL resummation. It is clearly a large effect for small p_T. Item (4) is not necessarily worth doing. We know that leading order SCET, like the parton

shower, is best when $p_T^{(1)} \gg p_T^{(2)} \gg \cdots \gg p_T^{(n)}$. So if two successive emissions occur at similar p_T's, the rate will be untrustworthy. However, a large p_T emission will appear as another jet, and so we really should do the higher-order matching to QCD, as in (1) and (2) to get the rate right. Item (5) is certainly important, but it may be prohibitively difficult to implement.

Our results were collected in the last two sections, and we have indicated how SCET might be used to construct an event generator. We have also investigated the uncertainties in traditional parton showers. For large values of p_T, these uncertainties arise from higher order in p_T/Q, which are not included due to the approximations required to derive parton showers. For small values of p_T on the other hand, the subleading logarithms which are not properly summed in the Sudakov factors give rise to large uncertainties as well. So, parton showers have relatively large uncertainties in most regions of phase space. Thus, while parton showers are very useful to populate phase space of events with many particles, it is very difficult to obtain results with small well-defined theoretical uncertainties. Since SCET is able to improve the precision in all regions of phase space, we showed how SCET might be used to produce events with controllable errors. Our prescription was to produce an initial m-parton distribution at high accuracy, including resummation of large logarithms within SCET, and then to use the parton shower and hadronization routines, which are constrained by unitary, to fill out the jets with particles. One can go further, for example, by using the properties of SCET, the accuracy of the shower routines could be improved, in principle, to any accuracy desired. Since effective field theories resum logs and are systematically improvable they have the potential to greatly improve our theoretical understanding of particle distributions.

ACKNOWLEDGMENTS

APPENDIX A: INTRODUCTION TO SCET

SCET is an effective theory containing only soft and collinear degrees of freedom, which can propagate over long distances. Since all long distance physics in massless QCD is determined by either soft or collinear particles, SCET is reproducing the long distance behavior of QCD, while all short distance physics can be encoded in short distance Wilson coefficients. SCET is essentially a simplified version of QCD in which all the IR degrees of freedom,

that is, the soft and collinear fields, are the same, but the UV structure is simplified. In particular, fields which are neither soft nor collinear are integrated out. The notation used in SCET emphasizes the nature of the SCET fields. Let n_μ be a lightlike direction $n_\mu = (1, \mathbf{n}_i)$, $\mathbf{n}^2 = 1$. Any four-vector can be decomposed with respect to n_μ and $\bar{n}_\mu = (1, -\mathbf{n}_i)$ as

$$p^\mu = \tfrac{1}{2}(\bar{n} \cdot p) n^\mu + \tfrac{1}{2}(n \cdot p) \bar{n}^\mu + p_\perp^\mu. \qquad (A1)$$

So we can define

$$\gamma_\perp^\mu \equiv \gamma^\mu - \tfrac{1}{2}\slashed{n} n^\mu + \tfrac{1}{2}\slashed{\bar{n}} \bar{n}^\mu, \qquad (A2)$$

and derive useful identities, such as

$$n \cdot \bar{n} = 2, \qquad \slashed{n}\slashed{n} = 0, \qquad \{\slashed{\bar{n}}, \slashed{n}\} = 4, \qquad \{\slashed{n}, \slashed{p}_\perp\} = 0, \qquad (A3)$$

$$p^2 = (n \cdot p)(\bar{n} \cdot p) + p_\perp^2. \qquad (A4)$$

We also denote the normalized four-vector in the direction of p by n_p. An operator $\mathcal{P}$ is often used to project out label momenta. For example,

$$\frac{1}{\bar{n} \cdot \mathcal{P}} \xi_n = \frac{1}{\bar{n} \cdot p} \xi_n. \qquad (A5)$$

A field is colliner to n if its momentum satisfies $|p_\perp| < \lambda \bar{n} \cdot p$, where λ is a small number giving the expansion parameter in SCET. The momentum of a collinear field scales like $(n \cdot p, \bar{n} \cdot p, p_\perp) \sim (\lambda^2, 1, \lambda)$, where we have used (A4) with $p^2 = 0$. A field is soft[4] if its momentum scales like $p \sim (\lambda^2, \lambda^2, \lambda^2)$. Note that the sum of two collinear momenta in the same direction is collinear, so collinear interactions are allowed. But if two fields are collinear to different directions, n_1 and n_2, they scale differently and interactions are forbidden. A Dirac fermion ψ_p with momentum p can be decomposed into collinear fermions ξ_n and $\xi_{\bar{n}}$ as

$$\psi_p = \frac{\slashed{n}\slashed{\bar{n}}}{4} \psi_p + \frac{\slashed{\bar{n}}\slashed{n}}{4} \psi_p \equiv \xi_n + \xi_{\bar{n}}. \qquad (A6)$$

The difference between ψ_p and ξ_n is that on shell, ψ_p satisfies $\slashed{p}\psi_p = 0$ while ξ_n satisfies $\slashed{n}\xi_n = 0$. When n is aligned with p, $\psi_p = \xi_{n_p}$, but in general $\slashed{p}\xi_n \neq 0$. The SCET Lagrangian is derived from the QCD Lagrangian by integrating out the small components $\xi_{\bar{n}}$ [2]. Then, using the scaling properties of the quarks and soft and collinear gluons, the Feynman rules are worked out as an expansion in λ. They can be found in [2–5].

SCET has the curious property that no information is lost when $\xi_{\bar{n}}$ is integrated out, even if only the first order

---

[4]Sometimes these fields are called ultrasoft, with soft denoting $p \sim (\lambda, \lambda, \lambda)$. These ''soft'' fields are not relevant for the current considerations as they cannot interact with either collinear or ultrasoft fields.

terms in the λ expansion are kept. There are a few ways to see this. First, note that $(\slashed{\bar{n}}\slashed{n})/4$ and $(\slashed{n}\slashed{\bar{n}})/4$ are projectors, in that they are orthogonal and complete. However, we can regain ψ_p from just ξ_n or $\xi_{\bar{n}}$ using the identity

$$\xi_{n_1} = \left(1 + \frac{\slashed{p}_\perp \slashed{\bar{n}}_1}{2\bar{n}_1 \cdot p}\right)\xi_{n_2}, \qquad (A7)$$

and that $\psi_p = \xi_{n_p}$. One should keep in mind that SCET is a boosted version of QCD [2], and any interactions between collinear fields in the same directions are thus given by full QCD. Whenever there are fields collinear to different directions, however, their interactions will be different from in QCD. It is in this situation that SCET is useful.

Since collinear fields in different directions do not interact with one another, there should be a separate collinear gauge invariance for each direction n. To ensure this gauge invariance, however, requires that each collinear fermion is multiplied by a collinear Wilson line, making the resulting field gauge invariant by itself

$$\chi_n = W_n \xi_n, \qquad W_n = \exp\left\{g_s \frac{\bar{n} \cdot A}{\bar{n} \cdot p_A}\right\}. \qquad (A8)$$

Each collinear fermion is therefore wrapped in collinear Wilson lines, and it is these collinear ''jets'' which are the basic building blocks of operators in SCET. For example, an operator with two jets would be

$$\mathcal{O}_2^{(n_1, n_2)} = \bar{\chi}_{n_1} \Gamma \chi_{n_2}, \qquad (A9)$$

where Γ is some tensor structure. Because n_1 and n_2 are different labels, no collinear fields can couple to both jets. Collinear gluons can couple one jet to itself, and soft gluons can be exchanged between jets. Diagrams in SCET are usually computed in $\overline{\text{MS}}$ dimensional regularization. It is also helpful to regulate IR divergences by giving the quarks and gluons small virtualities. These virtualities must drop out of physical calculations, and it is a helpful check on the theory to show that they do. Sample calculations can be found in [4]. Physical quark masses can easily be accounted for in SCET [49], but for simplicity we take all fields to be massless.

APPENDIX B: 3-PARTON KINEMATICS

For the three-parton final state, label the momenta of the quark, antiquark, and gluon p_q^μ, $p_{\bar{q}}^\mu$, and p_g^μ, respectively. There are two independent invariants we can construct. However, it is convenient to go between a number of kinematic variables. Let Q be the center-of-mass (COM) energy of e^+e^-. Then, we have

$$s \equiv (p_{\bar{q}} + p_g)^2 \equiv Q^2(1 - x_q),$$
$$t \equiv (p_g + p_q)^2 \equiv Q^2(1 - x_{\bar{q}}), \qquad (B1)$$
$$u \equiv (p_q + p_{\bar{q}})^2 \equiv Q^2(1 - x_g).$$

The invariants satisfy $s + t + u = Q^2$ and $x_q + x_{\bar{q}} + x_g = 2$. The x_q are half the energy of the corresponding particle, in the COM frame. We also define the four lightlike vectors pointing in the directions of the three particles as n_q, $n_{\bar{q}}$, and n_g. So

$$p_q^\mu = \frac{Q}{2} x_q n_q^\mu, \qquad p_{\bar{q}}^\mu = \frac{Q}{2} x_{\bar{q}} n_{\bar{q}}^\mu, \qquad p_g = \frac{Q}{2} x_g n_g^\mu. \tag{B2}$$

For each particle, we will also need the lightlike vectors pointing in the opposite direction

$$n_i = (1, \mathbf{n}_i) \Rightarrow \bar{n}_i = (1, -\mathbf{n}_i). \tag{B3}$$

The scalar products between different n_i can be obtained from (B1), and we also have

$$\bar{n}_i \cdot \bar{n}_j = n_i \cdot n_j, \qquad \bar{n}_i \cdot n_j = 2 - n_i \cdot n_j. \tag{B4}$$

We can also derive

$$\bar{n}_{\bar{q}} \cdot (p_q + p_g) = \frac{t}{Q}, \qquad n_{\bar{q}} \cdot (p_q + p_g) = Q \tag{B5}$$

and its permutations.

In the COM frame, the transverse momentum of the p_g or $p_{\bar{q}}$ with respect to p_q, p_q or $p_{\bar{q}}$ with respect to p_g, and $p_{\bar{q}}$ or p_g with respect to $p_{\bar{q}}$ are given, respectively, by

$$p_T^q = \frac{\sqrt{stu}}{x_q Q^2}, \qquad p_T^g = \frac{\sqrt{stu}}{x_g Q^2}, \qquad p_T^{\bar{q}} = \frac{\sqrt{stu}}{x_{\bar{q}} Q^2}. \tag{B6}$$

We will also define p_T as

$$p_T = \min(p_T^q, p_T^{\bar{q}}, p_T^g). \tag{B7}$$

Note that for $p_T \ll Q$,

$$p_T^2 \approx \frac{stu}{Q^4}. \tag{B8}$$

Finally, it is helpful when discussing splitting functions, to use variables defined with respect to only two partons. If we are considering the quark and gluon, then we can use the invariant mass of the pair, and the energy fraction of the gluon

$$t = Q^2(1 - x_{\bar{q}}), \qquad z = \frac{x_q}{x_g + x_q}. \tag{B9}$$

Some useful relations between these variables and the others are

$$x_{\bar{q}} = 1 - \frac{t}{Q^2}, \qquad x_q = z\left(1 + \frac{t}{Q^2}\right),$$
$$x_g = \left(1 + \frac{t}{Q^2}\right)(1 - z). \tag{B10}$$

[1] C. W. Bauer and M. D. Schwartz, Phys. Rev. Lett. **97**, 142001 (2006).
[2] C. W. Bauer, S. Fleming, and M. E. Luke, Phys. Rev. D **63**, 014006 (2000).
[3] C. W. Bauer, S. Fleming, D. Pirjol, and I. W. Stewart, Phys. Rev. D **63**, 114020 (2001).
[4] C. W. Bauer and I. W. Stewart, Phys. Lett. B **516**, 134 (2001).
[5] C. W. Bauer, D. Pirjol, and I. W. Stewart, Phys. Rev. D **65**, 054022 (2002).
[6] T. Sjostrand, Comput. Phys. Commun. **82**, 74 (1994).
[7] G. Marchesini, B. R. Webber, G. Abbiendi, I. G. Knowles, M. H. Seymour, and L. Stanco, Comput. Phys. Commun. **67**, 465 (1992).
[8] T. Gleisberg, S. Hoche, F. Krauss, A. Schalicke, S. Schumann, and J. C. Winter, J. High Energy Phys. 02 (2004) 056.
[9] M. A. Dobbs et al., arXiv:hep-ph/0403045.
[10] S. Mrenna and P. Richardson, J. High Energy Phys. 05 (2004) 040.
[11] S. Gieseke, P. Stephens, and B. Webber, J. High Energy Phys. 12 (2003) 045.
[12] S. Catani and M. H. Seymour, Nucl. Phys. **B485**, 291 (1997); **B510**, 503(E) (1997).
[13] M. Bengtsson and T. Sjostrand, Nucl. Phys. **B289**, 810 (1987).
[14] M. Bengtsson and T. Sjostrand, Phys. Lett. B **185**, 435 (1987).
[15] T. Sjostrand, S. Mrenna, and P. Skands, J. High Energy Phys. 05 (2006) 026.
[16] M. H. Seymour, Comput. Phys. Commun. **90**, 95 (1995).
[17] G. Miu and T. Sjostrand, Phys. Lett. B **449**, 313 (1999).
[18] E. Norrbin and T. Sjostrand, Nucl. Phys. **B603**, 297 (2001).
[19] S. Catani, F. Krauss, R. Kuhn, and B. R. Webber, J. High Energy Phys. 11 (2001) 063.
[20] L. Lonnblad, J. High Energy Phys. 05 (2002) 046.
[21] F. Krauss, J. High Energy Phys. 08 (2002) 015.
[22] A. Schalicke and F. Krauss, J. High Energy Phys. 07 (2005) 018.
[23] S. Hoche, F. Krauss, N. Lavesson, L. Lonnblad, M. Mangano, A. Schalicke, and S. Schumann, arXiv:hep-ph/0602031.
[24] S. Catani, Y. L. Dokshitzer, M. Olsson, G. Turnock, and B. R. Webber, Phys. Lett. B **269**, 432 (1991).
[25] T. Kinoshita, J. Math. Phys. (N.Y.) **3**, 650 (1962).
[26] T. D. Lee and M. Nauenberg, Phys. Rev. **133**, B1549 (1964).
[27] S. Frixione and B. R. Webber, arXiv:hep-ph/0601192.
[28] M. Dobbs, Phys. Rev. D **65**, 094011 (2002).
[29] B. Potter and T. Schorner, Phys. Lett. B **517**, 86 (2001).
[30] J. C. Collins and F. Hautmann, J. High Energy Phys. 03 (2001) 016.
[31] M. Kramer and D. E. Soper, Phys. Rev. D **69**, 054019

(2004).

[32] D. E. Soper, Phys. Rev. D **69**, 054020 (2004).

[33] Z. Nagy and D. E. Soper, J. High Energy Phys. 10 (2005) 024.

[34] G. Davatz, F. Stockli, C. Anastasiou, G. Dissertori, M. Dittmar, K. Melnikov, and F. Petriello, J. High Energy Phys. 07 (2006) 037.

[35] S. Frixione, P. Nason, and B. R. Webber, J. High Energy Phys. 08 (2003) 007.

[36] A. V. Manohar and I. W. Stewart, arXiv:hep-ph/0605001 [Phys. Rev. D (to be published)].

[37] A. V. Manohar, Phys. Rev. D **68**, 114019 (2003).

[38] C. W. Bauer, C. W. Chiang, S. Fleming, A. K. Leibovich, and I. Low, Phys. Rev. D **64**, 114014 (2001).

[39] R. K. Ellis, D. A. Ross, and A. E. Terrano, Nucl. Phys. **B178**, 421 (1981).

[40] R. K. Ellis, D. A. Ross, and A. E. Terrano, Phys. Rev. Lett. **45**, 1226 (1980).

[41] K. Fabricius, I. Schmitt, G. Schierholz, and G. Kramer, Phys. Lett. B **97**, 431 (1980).

[42] S. Frixione, Z. Kunszt, and A. Signer, Nucl. Phys. **B467**, 399 (1996).

[43] W. T. Giele and E. W. N. Glover, Phys. Rev. D **46**, 1980 (1992).

[44] W. T. Giele, E. W. N. Glover, and D. A. Kosower, Nucl. Phys. **B403**, 633 (1993).

[45] A. Gehrmann-De Ridder, T. Gehrmann, and E. W. N. Glover, Nucl. Phys. **B691**, 195 (2004).

[46] C. Anastasiou, K. Melnikov, and F. Petriello, Phys. Rev. D **69**, 076010 (2004).

[47] C. Anastasiou, K. Melnikov, and F. Petriello, Phys. Rev. Lett. **93**, 032002 (2004).

[48] G. Sterman and S. Weinberg, Phys. Rev. Lett. **39**, 1436 (1977).

[49] A. K. Leibovich, Z. Ligeti, and M. B. Wise, Phys. Lett. B **564**, 231 (2003).